1998

Hydrothermal aging of zeolite-based catalysts

Joongjai Panpranot
West Virginia University

HYDROTHERMAL AGING OF ZEOLITE-BASED CATALYSTS

By

Joongjai Panpranot

A THESIS

Submitted to

The College of Engineering and Mineral Resources

at

West Virginia University

in partial fulfillment of the requirements

for the degree of Master of Science

in

Chemical Engineering

Department of Chemical Engineering

Morgantown, West Virginia

1998

ABSTRACT

In this study the RE-USY (Davision GO-40) FCC catalyst, a composite of RE-USY zeolite and alumina-silica gel matrix, was treated hydrothermally under simulated FCC regenerator conditions in a laboratory scale fluidized bed. Fresh and steam-aged catalysts were characterized by surface area reduction using the nitrogen BET and t-Plot surface area methods. The surface morphology was apparent from the scanning electron photomicrographs. An irreversible deactivation kinetic model developed earlier by Gardner

$$[(S_0\text{-}S)/S_0]^{ns} = K_s\, t$$

was applied to account for changes of surface area of the zeolite component as a function of time on stream, temperature and steam partial pressure. The kinetic parameters, K_s, the apparent global zeolite hydrothermal stability rate constant and n_s, a constant which was determined to be a function of steam partial pressure for a given temperature were determined and compared to those of H-USY (Davision Octacat) FCC catalyst.

An effect of rare-earth exchange on deactivation kinetics was observed. The RE-USY was found to exhibit greater hydrothermal stability than the H-USY determined by the smaller hydrothermal stability rate constant, K_s, and the smaller n_s. The presence of rare-earth ions in the zeolite was suggested to prevent extraction of aluminum atoms which caused the hydrothermal destruction of zeolite framework.

ACKNOWLEDGEMENT

First of all, I would like to express my deepest gratitude towards my advisor, Prof. Edwin L. Kugler. He advised, guided and helped me throughout my research. I am also thankful for my committee members, Prof. Dady B. Dadyburjor and Prof. Charter D. Stinespring for reviewing my work. The design of the system by Todd H. Gardner is also acknowledged.

I would like to thank Prof. Yon Rojanasakul from School of Pharmacy, Mr. Jim P. Poston and Mr.George T. Lee, from the United States Department of Energy for performing the scanning electron microscope analysis. I also owe my achievements to my parents and my friends, who provided encouragement and support throughout this period and I am dedicating my work to them.

TABLE OF CONTENTS

LIST OF TABLES

LIST OF FIGURES

NOMENCLATURE

Symbol	Explanation
Activity	conversion/(100%conversion)
E_A	Apparent activation energy for zeolite hydrothermal stability, J/mol
EDTA	Ethylenediamine tetraacetic acid
EFAL	Extra-framework aluminum species
FCC	Fluid Catalytic Cracking
FCCU	Fluid Catalytic Cracking Unit
HPLC	High performance liquid chromatography
H-USY	Hydrogen ultrastable Y zeolite
K_s	Apparent global hydrothermal stability rate constant, s^{-1}
k_{s0}	Pre-exponential factor, s^{-1}
MAT	Microactivity test
n_s	A constant which is a function of steam partial pressure
P_{steam}	Steam partial pressure, atm
R	Gas constant, 8.314 J/(mol.K)
RE-USY	Rare-earth exchanged ultra stable Y zeolite
RE-Y	Rare-earth exchanged Y zeolite

Symbol	Explanation
S	Zeolite surface area, m^2/g
S_0	Initial zeolite surface area, m^2/g
SA	Surface area, m^2/g
SEM	Scanning electron microscope
T	Temperature, Kelvin
t	time, hours

1.0 INTRODUCTION

Fluid Catalytic Cracking is an important refining process to upgrade heavy hydrocarbons to high valued products. Over its 50-year history, this process has continuously undergone changes and major improvements related to the technology as well as the catalyst (1). Approximately 1,100 tons of catalyst is manufactured every day to be used worldwide in over 200 Fluid Catalytic Cracking Units (2). Usually, the catalysts are a mixture of faujasite (Y) zeolite and amorphous silica-alumina materials and may contain some additional additives to adjust their properties.

1.1 Zeolites

Certain aluminosilicates were first termed zeolites more than two centuries ago. Zeolites occur naturally and are produced synthetically in a variety of crystalline forms. Zeolites find their largest scale application in being used as major components in cracking catalysts since the Mobil Oil Corp. introduced the first zeolite-containing cracking catalyst in the early 1960's (3). It has shown to have an activity for cracking gas oil more than 100 times as great as amorphous silica-alumina catalysts which were used in the earlier cracking processes (4).

The unusual high activity and selectivity of zeolites are known to be related to their extremely fine uniform pore structures (3). The pore size distribution for a zeolite compare to other adsorbents (a typical silica gel and activated carbon) is illustrated schematically in Figure 1.

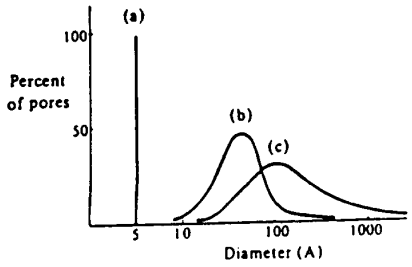

Figure 1: Distribution of pore sizes in microporous adsorbents (a) dehydrated zeolite (b) typical silica gel (c) activated carbon (4).

These uniform pores of zeolites will completely exclude molecules which are larger than their diameter. This is the reason that a zeolite sometimes is named “molecular sieve”. According to Breck (4), structurally zeolites are “framework” aluminosilicates, which are based on an infinitely extending three-dimensional network of AlO_4^- and SiO_4 tetrahedra linked to each other by sharing all of the oxygen atoms. The negative charge associated with the framework aluminum ions is neutralized by metal cations which usually are Group I and Group II elements. Some of these cations must be able to undergo reversible ion exchange (3). Water molecules fill the remaining volume of channels and interconnected voids or cages in the framework of zeolites. This intracrystalline “zeolitic” water in many zeolites is removed continuously and reversibly. The unit cell formula is usually written as

$$M^{+}_{x/n}[(AlO_2^-)_x(SiO_2)_y].wH_2O$$

where M is the cation of valence n, w is the number of water molecules and the ratio y/x usually has values of 1-5 depending upon the structure. The sum x+y is the total number of tetrahedra in the unit cell (4). The cations are usually sodium ions (Na^+) as the typical reactants of synthetic zeolites are sodium aluminate, sodium hydroxide and aqueous colloidal silica sol (5).

The primary building blocks of all zeolites consist of a tetrahedron of four oxygen anions surrounding a small silicon or aluminum cation are shown in Figure 2.

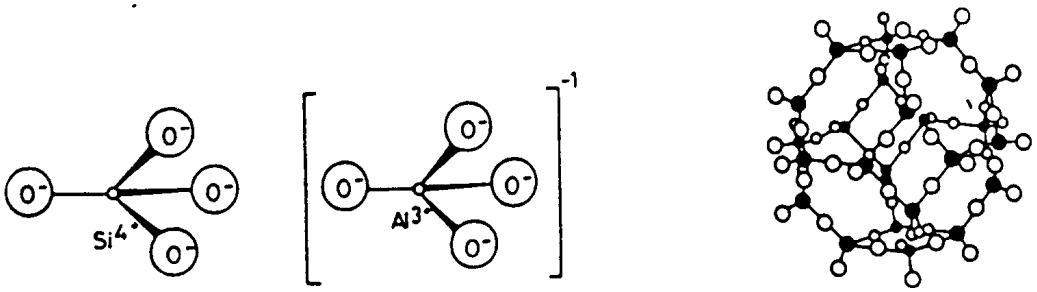

Figure 2: Silica and alumina tetrahedron (4)

The primary building blocks of zeolite can be combined in many arrays with sharing of O atoms (6). This arrangement results in more complicated crystalline frameworks. The number of oxygen atoms per ring determines zeolite pore diameters. The size of the aperture also depends on the nearby cations. When the Na cations mentioned above are exchanged for other cations, the chemical and physical properties of the zeolite are altered. A large cation may partially block supercage openings and exclude larger reactant molecules (7). The most common zeolite structure is that of faujasite or synthetic X and Y zeolites. Its main pore structure is found to be large enough (7.4 angstroms) to admit large hydrocarbon molecules such as naphthalene (5). X and Y zeolites have the same structure, differing only in the ratio of silicon to aluminum atoms present in each. For X, $1.0 \leq$ Si/Al ≤ 1.5. For Y, $1.5 \leq$ Si/Al ≤ 3.0 (8). The three-dimensional chain-type structure of Y zeolite is represented in Figure 3.

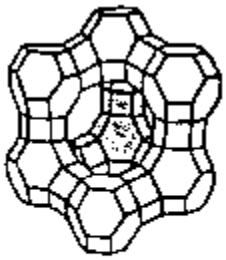

Figure 3: Structure of Y-zeolite (8)

1.2 Fluid Catalytic Cracking (FCC) Process

1.2.1 Fluid Catalytic Cracking Unit (FCCU)

Since the start-up of the first commercial Houdry fixed-bed plant in 1936, the technology of catalytic cracking has seen many innovations: from moving bed cracking, fluid-bed catalytic cracking (dense bed) to the present riser and residue FCC processes (9,10). A typical FCC unit consists of a riser reactor, where catalytic cracking of hydrocarbon occurs, and a fluidized bed regenerator, where spent catalysts are regenerated. Schematically, the FCC unit is shown in Figure 4.

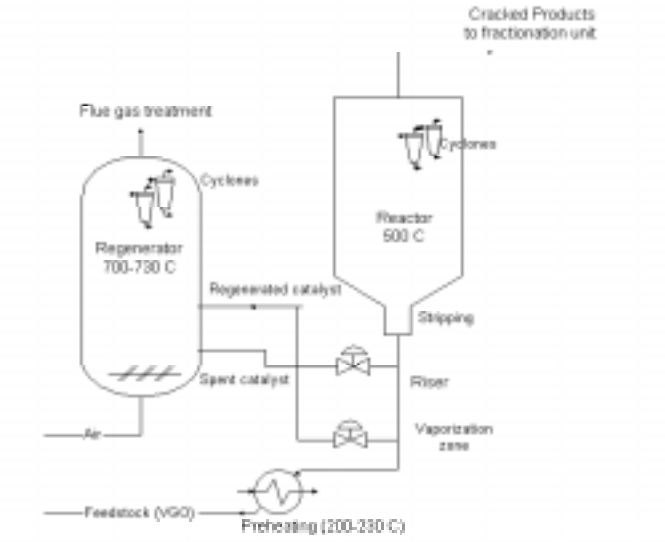

Figure 4: A typical FCC Unit (1)

A preheated vacuum distillate feed is introduced to the unit at the bottom of the riser. Feed is contacted with the catalyst which is coming from the regenerator at high temperature (700°C), and immediately is vaporized and cracked. At the riser exit, catalyst is recovered in two cyclones connected in series and the hydrocarbon vapors are separated. At the lower part of the reactor is the stripper for spent catalyst. In the regenerator, spent catalyst is fluidized by combustion air. High temperature combustion removes any coke deposited on the catalyst to carbon dioxide (CO_2). The standard operating conditions for the reactor and regenerator are summarized in Table 1.

Table 1: Standard FCC operating conditions (1,3,11).

Riser Reactor		Fluidized Bed Regenerator	
Temp., °C	510-550	Temp., °C	650-800
Pressure, atm	1.5-3	Pressure, atm	3.5
Cat-to-Oil ratio	6	Sup. gas vel., cm/s	60
Gas residence time, s.	5-7	CO/CO_2 mol ratio	0.7-1.3: 1
		Solids residence time, s.	30
		Coke content, wt%	
		at entrance	0.8
		at exit	0.1
		Steam pressure, atm	0.7

1.2.2 FCC Catalyst

FCC catalyst is a complex composite acid solid with two main components: zeolite, which is the main active acidic agent, and matrix. It is usually in the form of microspheres with 50-70 μm average diameters. The microstructure of FCC catalyst is shown in Figure 5.

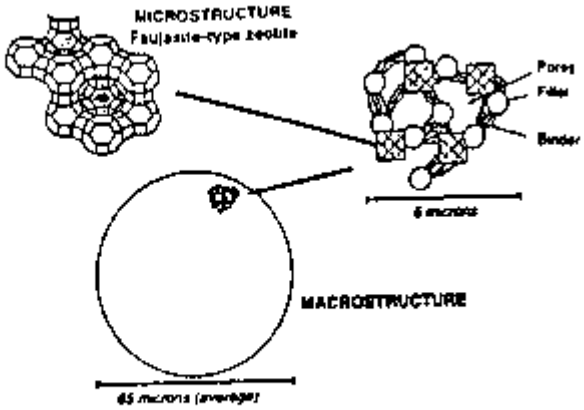

Figure 5: FCC catalyst components (Schematic) (1).

The matrix is composed of kaolin clay filler and silica or alumina binder. The major role of matrix is to bond the zeolite particles together and also to form a diffusion medium for the oil molecules. Another role is to act as a diluent media to moderate zeolite activity (3). The zeolite content in FCC catalyst ranges between approximately 10-50% by weight.

According to the desired selectivity, the following forms of Y zeolites can be introduced into FCC catalysts (1). Rare earth exchanged Y zeolite (REY) with high hydrogen transfer properties gives high yields of gasoline. The hydrogen form of ultra-stable Y zeolite (H-USY) is a zeolite without any rare earth, with a low acid density that results in lower gasoline yield but with much better octane and lower coke yield. RE-H-Y and RE-H-USY zeolites have intermediate properties between the previous two zeolites.

1.3 Deactivation of FCC catalysts

As soon as it is introduced into the unit, the catalyst undergoes significant aging, due partly to the severe conditions in the regenerator and partly to the effect of the metallic contaminants in feed. To maintain catalyst activity, one to several percent of the total inventory of the facility is replaced by fresh catalyst (several tons per day) (1).

In this thesis, the study will be focused on hydrothermal aging of zeolite-containing catalyst in simulated regenerator conditions. The presence of steam at high temperature (about 650-780°C) within the first hour rapidly causes an irreversible loss of the specific surface area of the catalyst, including both zeolite and silica-alumina matrix.

For silica-alumina, surface area reduction is due to sintering of the particles, increasing their size (1). The change in zeolite is different. Deep and complex modifications of the zeolites framework occur (2,12,13,14,15). They include modification of the chemical composition of the framework, formation of **E**xtra-**F**ramework **Al**uminum species (EFAL), formation of atomic vacancies and large cavities (a few hundred angstroms in diameter) in the framework, and finally slow and progressive collapse of the zeolite structure. These phenomena are known as the results from 'dealumination' of zeolite lattices. It is well documented that the existence of Al-O-Al fragments in zeolite lattices is virtually excluded (16) (so called 'Loewenstein's rule'), consideration of any zeolite structural changes are based on this rule. A number of researchers have investigated dealumination mechanism of the zeolite catalysts through various processes (14,15,17,18,19,20). However no certain models for dealumination have been proposed so far (19).

Above 500°C, aluminum atoms which are associated with protons are progressively extracted from their tetrahedral acidic sites and deposited in the pores in the form of oxyhydroxides, migrate and some recombine. The degree of dealumination is dependent on temperature (12). The empty aluminum atom vacancies may be filled by a local recrystallization of the zeolite framework (14,15,21) or reoccupied by silicon atoms that migrate from either the noncrystalline fraction or the framework itself (17,18,19). On the whole, the silicon enriched framework improves its stability. The aluminum depletion corresponds to a decrease in the number of acidic sites which results in decreasing of activity. However, in the regenerator (700-750°C), the aluminum extraction process is faster than the silica reinsertion, culminating in a widespread collapse of zeolite structure (1).

2.0 THESIS STATEMENT

The purpose of this study was to describe the irreversible deactivation kinetics of RE-USY zeolite in the RE-USY (Davison GO-40) FCC catalyst in the form of surface area changes as a function of time, temperature and steam partial pressure. In a prior study, Gardner (11) developed a new structural kinetic model for the hydrothermal deactivation of H-USY zeolite in the H-USY (Davison Octacat) FCC catalyst under simulated regenerator conditions. The deactivation was expressed in the form of the following equation

$$[(S_0-S)/S_0]^{ns} = K_s\, t$$

where S_0 is the initial zeolite surface area, S is the zeolite surface area at time t, t is time on stream, K_s is an apparent global hydrothermal stability rate constant, and n_s is a constant which was determined to be a function of steam partial pressure at a given temperature.

The same kinetic model was applied to the deactivation of RE-USY zeolite in the RE-USY (Davison GO-40) FCC catalyst. The kinetic parameters, K_s and n_s were calculated and compared to those of H-USY (Davison Octacat) FCC catalysts. Since the aluminum atom associated with rare-earth ions is known to be more firmly held in the zeolite framework (1), the effect of rare-earth ion exchange was ascribed to the difference in hydrothermal stability of the two zeolite-based catalysts. The investigation also included how hydrothermal conditions affect the surface area of matrix components of the RE-USY zeolite catalyst.

3.0 LITERATURE REVIEWS

In this chapter, literature reviews have been made for 1) the steam aging procedure of zeolite catalysts 2) proposed mechanism of zeolite dealumination 3) kinetic modeling of zeolite catalyst structural change under laboratory hydrothermal conditions and 4) determination of zeolite surface area.

3.1 Hydrothermal Aging Procedures

The hydrothermal aging also known as steam aging or steam treatment of cracking catalyst is a useful technique to examine zeolite structural changes when exposed to hydrothermal conditions with the assumption of no other influences such as contaminant metals levels, catalyst addition rate, etc. A hydrothermal aging procedure more severe than that in the actual FCCU has been used to accelerate the hydrothermal aging of the catalysts. Structural changes of the catalyst caused by steam aging include reducing surface area, microporosity and crystallinity which are attributed to decreasing cracking activity and changing selectivity of the cracking catalyst (22).

ASTM method D4463-91, “Standard guide for steam deactivation of fresh fluid cracking catalysts” (25) provided a standardized testing method for deactivating fresh catalytic cracking catalysts using either fixed or fluid bed steaming reactors under selected temperatures between 700-850 °C for 4-6 hours. While an ASTM procedure for steam aging does exist, no laboratory was found to practice it in total (24). Instead, each laboratory has developed individualized steaming procedures that best suit their needs. At least six steam aging procedures are known to be specifically used.

McElhiney (25) proposed a single specific condition for steam aging cracking catalyst at 815 °C with 100% steam and ambient pressure for 5 hours. This method had the purpose to reduce the structural and catalytic properties of certain fresh commercial catalysts to equilibrium levels in a short period of time for further evaluation using microactivity test (26). This simple steam aging procedure has been found capable of reducing the acidity of the fresh FCC under study to those that the same FCC exhibit after being used in an actual FCCU. However, this method provides insufficient data to describe hydrothermal stability of a cracking catalyst.

Keyworth and co-workers (29) proposed age distribution steaming involved blending portions of catalyst which had been steam aged for 2, 4, 6 and 8 hours at 795 °C and ambient pressure. The blending of catalysts reportedly simulated the mixture found in the actual equlibrated catalysts. Nevertheless, the unequal weight fractions of aged catalysts in the actual FCCU weaken this procedure’s merit.

Mclean and Moorehead (28) reportedly found an accurate simulation of certain commercial equlibrated catalysts by blending of five weight percent fresh catalyst with steamed aged catalyst. The steam aging conditions were 760-816°C and 100 % steam partial pressure at ambient pressure for 5-60 hours.

According to an evaluation of fluid cracking catalysts, made by Mclean and Moorehead in 1989 (24), it has been stated that a number of laboratories used a fixed time and temperature ranges from 760-815°C to achieve a range of deactivated samples. The aged samples obtained were evaluated in a microactivity test (MAT) unit. Zeolite surface area and unit cell size as functions of temperature were shown in plots. Also in Mclean and Moorehead study (24), the temperature was fixed and the time was varied from 5-60 hours with a preferred time of 4-24 hours. Hydrothermal stability curves were constructed.

Recently, Gardner (12) studied irreversible deactivation kinetics of H-USY and H-ZSM-5 zeolites with a steam aging technique. The effects of steam partial pressure, temperature and time on zeolite hydrothermal stability have been investigated. Catalyst performance was described in a form of a kinetic model of zeolite surface area reduction as a function of aforementioned three variables.

Variations of these steam aging methods have also been reported. Some laboratories tested all catalysts at constant conversion typical of what equilibrium catalysts exhibit in the actual FCCU by adjusting steaming severity (24). Rather than steam aging to a constant conversion, some workers have deactivated catalysts to other measurable physical properties. A

comparison was made based on selectivity data. The need to have more than one steaming procedure for extremely different catalysts has been proposed by Magee et al. (29). It is more practical to adjust steaming severity to such that the steamed properties for groups of catalysts are representative of what will be observed commercially than to have a single steaming procedure for every catalyst.

In addition to the various steam aging methods discussed, two techniques for introducing catalysts into laboratory reactors have been used. Some workers prefer slow heating of the catalyst while others practice "shock" treatment.

For slow heating method (12), the catalyst was introduced into the reactor at room temperature and then temperature was increased at a rate of 5 K min^{-1} to treatment temperature under a dry nitrogen flow of 100 ml/min. The other method was described as "shock" treatment, where the catalyst was introduced directly to a pre-heated steam environment (24).

Gas-solid contacting schemes had also been taken into account for steam aging procedures. The type of gas-solid contacting used produced differing steam aged catalyst properties (30). The work done by Kerr (31) reported two methods to fill a ceramic "boat" with catalyst sample. These two methods had also been reported by Basacek and Patzelova (32).

The first method described steam aging under "deep bed" conditions (31). An aged distribution within the sample was formed due to the variation in gas-solid contacting along the depth of the bed. With water or ammonia molecules liberated during this treatment, self-steaming of the lower layers of the zeolite sample occur.

The second method described steam aging under “shallow bed” conditions (31). A thin layer of zeolite catalyst sample was filled in the ceramic “boat”. Shallow-bed steam aging provided good gas-solid contacting and perhaps result in a more homogeneously deactivated sample. This technique was found to be especially useful with extremely fine zeolite particles when the fluidized bed method was unsuitable.

In ASTM method D 4463-91, “Standard guide for steam deactivation of fresh cracking catalysts” (23), both fixed and fluidized bed reactors have been employed. The fluidized bed however is believed to provide the most homogeneous gas-solid contacting for cracking catalyst. However slugging phenomena may occur in a gas-fluidized bed under certain conditions (33).

3.2 Mechanism of Zeolite Dealumination

Dealumination of zeolite structure, which leads to crystal defects, creation of a secondary pore system and formation of extra-framework aluminum, has been conducted in numerous studies through different processes. As of industrial importance, dealumination methods involve calcination and hydrothermal treatment, strong acid leaching and silicon tetrachloride treatment. Other dealumination processes, e.g. the use of F_2 or $CrCl_3$ are not yet of industrial practice (7).

Kerr (14) treated NaY zeolite with an acidic solution of ethylenediamine tetraacetic acid (EDTA) to obtain a homogeneously dealuminated zeolite sample. His proposed dealumination mechanism was that each missing aluminum atom was replaced by four hydrogens bonding to the oxygen atoms of the vacated tetrahedron. The four hydroxyl products each bonded to silicon

were believed to condense to yield water and form Si-O-Si bonds upon heating. The new Si-O-Si bond has been found to improve the framework thermal stability. The optimum removal of aluminum for thermal stability was in the range of 25-50%.

Gallezot, Beaumont and Barthomeuf (15) followed the same procedure as in Kerr's work by using EDTA to remove aluminum atoms of NaY zeolite and derive a homogeneously dealuminated zeolite sample. The results obtained from x-ray powder diffraction showed no significant change of the occupancy factor of the zeolite framework atoms. This was interpreted as the vacancies in the framework left by homogeneously removed aluminum atoms were refilled through a local crystallization process so that the over all structure was preserved. The process was found to involve the formation of new SiO_4 tetrahedra. Two possible sources of silicon atoms were either from siliceous impurities, which are often present in synthetic zeolites or from the zeolite framework itself.

Sulikowski, Karge and Mishin (20) proposed an improved method for dealumination of faujasite-type zeolites with silicon tetrachloride treatment. With this method, in contrast to hydrothermal treatment or acid leaching, the direct substitution of the framework aluminum by silicon atoms was reported. However, the reaction has a limited temperature up to about 700 K. Beyond this point, higher degree of dealumination cannot be obtained due to the deposition of the reaction product $NaAlCl_4$ in the pore system. The presence of aluminum extraframework species was revealed by ^{27}Al MAS NMR spectrometry.

Wang, Giannetto and co-workers (34) studied the kinetics of dealumination by hydrothermal treatment of NH_4NaY zeolite and using of x-ray powder diffraction to characterize the variations of the crystallinity. A three step mechanism for dealumination was proposed as follows: 1) deammoniation at low temperature 2) hydrolysis of various Si-O-Al bonds and 3) migration of the aluminum species and reinsertion by silicon atoms.

Klinowski, Thomas, Fyfe and Gobbi (35) dealuminated NaY zeolite samples using various methods including steaming and acid leaching. High resolution magic-angle-spinning solid-state ^{29}Si and ^{27}Al NMR spectroscopy was used to monitor structural changes within the zeolite framework. The results showed that the empty aluminum atom vacancies were partially reoccupied by silicon atoms which not only came from noncrystallization fractions of zeolite but also from the local recrystallization of the framework silicon atoms.

In a recent work of Alvarez et al. (19), charge transfer molecular dynamics simulations (CTMD), a new powerful tool of computer simulation technique has been used to investigate the structural and dynamic properties of zeolite. The results have been found in agreement with those of aforementioned works in such a way that each extracted aluminum atom was replaced by four hydrogens bonding to the oxygen atoms of the vacated tetrahedron. Further heat treatment led to dehydroxylation of the nests of four hydroxyls and to the formation of new Si-O-Si bonds accompanied by some disordering of the framework. The simulation also revealed the instability of the Al-O bonds, leading to a major distortion of the structure which may result in the collapse of the structure upon total dealumination.

Although these facts have often been reported, no clear model has been proposed so far to explain the observed results (21). Some complex questions related to dealumination of zeolite catalysts are still not yet answered such as whether or not the aluminum extraframework forms some additional compound as alumina for instance, and if so, whether these clusters interact with the zeolite framework or have any effect on catalyzed reaction.

3.3 Modeling of Zeolite Structural Changes Due to Steam Aging

Kinetic modeling of zeolite structural changes derived from experimental data fitting has been used as a powerful tool to examine a catalyst's structural stability and to predict its behavior under different conditions. Such modeling, historically, has been accomplished through the measurement and correlation of zeolite surface area, percent crystallinity, the unit cell dimension and activity/selectivity to temperature, steam partial pressure and time (11).

In an early investigation of Schalaffer, Adams and Wilson (36) in 1965, an attempt was made to assess silica and alumina catalyst structural stability toward steam aging. The changes in catalyst surface area was described by an empirical equation of the power law form

$$dS/dt = kS^n$$

where S is the catalyst's surface area, t is time, n and k are constants at any given set of aging conditions. This simple model is somewhat limited in that steam partial pressure was not included as a variable within this equation.

An empirical correlation of observed changes in zeolite crystallinity as a function of steam aging parameters has been developed by Chen, Mitchell, Olson and Peirine (37). This correlation is

$$\ln A/A_0 = -ke^{(-E/RT)} p^n t^m$$

where A_0 is the catalyst's initial crystallinity, A is the crystallinity observed at time t, k is a pre-exponential factor, E is an apparent activation energy, p is the steam partial pressure, t is time on stream, R is the gas constant and T is absolute temperature. As stated by the authors, this correlation failed in the low partial pressure range.

Chester and Stover (38) studied kinetic steam aging of three FCC catalyst samples: semi-synthetic, clay and clay-gel. The three catalysts were deactivated by steam treating with 100% steam, 0 psig in a fluidized bed at various temperatures (671-843°C). A deactivation rate constant is represented empirically by the sum of two independent first-order decays of the form

$$k_d(T) = A_m e^{-Em/RT} + A_z e^{-Ez/RT}$$

Here k_d is an apparent deactivation rate constant, A_M and E_M are pre-exponential and apparent activation energy parameters for changes in the matrix components, A_Z and E_Z are pre-exponential and apparent activation energy parameters for changes in zeolite activity, R is the gas constant and T is absolute temperature.

Suckow, Lutz, Kornatowski, Rozwadowski and Wark (39) developed a global structural kinetics model to account for a loss in crystallinity of NaCa5A binder-free zeolite catalysts as a function of time, temperature and steam partial pressure. The samples were treated hydrothermally for periods up to 72 hours in a shallow bed with temperature ranges of 843-953 K and 20-100% steam partial pressure. The model was described as

$$\ln Z/Z_0 = -k_0 e^{(-EA/RT)} (1+\varpi)^{\alpha} t$$

where Z_0 is the zeolite's initial crystallinity, Z is the crystallinity observed at time t, k_0 is a pre-exponential factor, E_A is an apparent activation energy, w is the normalized water concentration, t is time on stream, α is a constant, R is gas constant, and T is absolute temperature. The model as pointed out by the authors tended to have poor prediction capabilities of zeolite structural changes at low steam partial pressure. The model did not include data for times less than three hours.

Blasco, Royo, Monzon and Santamaria (40) developed a sintering kinetic model for a commercial Cr_2O_3/Al_2O_3 catalyst based on in-situ observed changes in activity as a function of temperature and time. The data used for derivation were obtained in a fixed-bed reactor under cyclic operation. With coke-free conditions, catalyst activity loss was assumed to be due to sintering. The sintering kinetic model developed is

$$-da_0/dt = 0.147 \exp(-73{,}600/RT)\, a_0^{2.2}$$

where a_0 is initial activity of the catalyst, t is time, R is the gas constant and T is absolute temperature. The value 0.147 is the rate constant with the unit sec^{-1}, 73,600 J/mol is an apparent activation energy and 2.2 is a constant. This sintering kinetic model was probably an original form of the surface area reduction kinetic model of zeolite catalyst.

Gardner (11) developed a simple surface area reduction model to describe the changes in surface area as a function of time, temperature and steam partial pressure of H-USY zeolite catalysts. The steam aging conditions were simulating those of the refinery FCC regenerator. Temperature was in the range of 650-800 °C and steam partial pressures of 0-1 atmospheres. The deactivation was expressed in the form of following equation

$$[(S_0\text{-}S)/S_0]^{ns} = k_{s0}\, e^{(-Ea/RT)}\, t$$

where S_0 is the initial surface area, S is the surface area at time t, E_a is an apparent activation energy for zeolite hydrothermal stability, n_s is a constant which was determined to be a function of steam partial pressure at a given temperature, k_{s0} is a pre-exponential factor, t is time on stream, R is the gas constant and T is absolute temperature. This simple surface area kinetic model provided a useful measure of a zeolite catalyst's hydrothermal structural stability. It has also been suggested by the author that the model can be used as a quantitative analytical tool to compare one faujasite-type zeolite catalyst's hydrothermal stability to another's.

3.4 Determination of Catalysts Surface Area

Surface area of FCC catalysts was measured by nitrogen adsorption using the well-known BET (the Brunauer-Emmett-Teller) method. The theoretical principles and experimental procedures are described briefly in the following.

3.4.1 Physical adsorption of a gas by a solid

It is known that the quantity of gas taken up by a sample of solid depends on the temperature, the pressure of the vapor, and the nature of both the solid and the gas. The plot between the quantity of gas adsorbed on a particular solid at a fixed temperature and the relative vapor pressure (P/P^o), where P^o is saturated vapor pressure, is known as the "adsorption isotherm". Tens of thousands of adsorption isotherms have been literally reported on a wide variety of solids (41). Nevertheless, those isotherms may be grouped into five categories, according to the physical properties of the adsorbent (the solid). These have the names type I for microporous solids, type II for non-porous solids and type IV for meso-porous solids. Type III and V relate to the special behavior of water adsorption.

3.4.2 Surface area of catalysts

For evaluation of both surface area and pore size distribution of a solid from a single isotherm, nitrogen is found to be a suitable adsorbate. It meets the conditions that the adsorbate be chemically inert towards solid and that saturation vapor pressure, P^o, at the working temperature be large enough to allow the accurate measurement of the relative pressure over a reasonably wide range (41).

Determination of surface areas of catalysts usually follows the ASTM D3663 (standard test method for surface area of catalysts) (42). The surface area of a catalyst is determined by

measuring the volume of nitrogen gas adsorbed at various low-pressure levels by the catalyst sample. Pressure differentials caused by introducing the degassed catalyst surface area to a fixed volume of nitrogen in the test apparatus are measured and used to calculate BET surface area (41). If the catalyst contains micropores—pores which are no more than a few molecular diameters in width--this will result in a distortion of the isotherm, especially at low relative pressures. In this thesis, the investigation is made for a composite type of catalyst, which consisted of zeolite and alumina-silica gel matrix. The zeolite portion of the catalyst is characterized by micropores. The procedure to determine zeolite area is described in ASTM D4365 (standard test method for determining zeolite area of a catalyst) (43). This procedure is the same as Test Method D3663, that gives total surface area, but extends the pressure range to permit calculation of matrix surface area by the t-plot method.

4.0 EXPERIMENTAL METHODS

This chapter provides specifications of the catalyst, the test apparatus, the procedure to steam age the catalyst samples as well as the analytical equipment and method used to characterize changes of zeolite and matrix surface area.

4.1 Fresh Properties of the RE-USY (Davison GO-40) FCC Catalysts

The FCC catalyst samples used in this investigation were commercial non-promoted grades fluid catalytic cracking catalysts “GO-40” provided by W.R.Grace, Davison Chemical Division, Baltimore, Maryland. Approximate compositional analysis of the catalysts as provided by the Material Safety Data Sheet are shown in Table 2.

Table 2: The RE-USY (Davison GO-40) FCC Catalyst Compositions

	Wt%		Wt%
Alumina (Al_2O_3)	20-60	Sodium Oxide (Na_2O)	0-1.0
Silica (SiO_2)	40-80	Titania (TiO_2)	0-1.0
Rare Earths (Re_2O_3)	0-10	Total Volatile	2-16
Sulfate (SO_4)	0.1-2.5	Quartz (SiO_2)	1.0

The typical physical and chemical properties of the catalysts are as follows:

Appearance: Off-white fine powder (microspheroides)

pH in 5% slurry: 3-6

Odor: none

Specific gravity: Approximately 2.1

Bulk Density: 0.45 gram/cc to 1 gram/cc

Solubility in water: Nil.

Stability: Stable

Reactivity: React with HF, otherwise inert

Fire & Explosion data: non-flammable, will not explode

Figure 6 is the scanning electron photomicrographs, which show the surface morphology of the fresh RE-USY (Davison GO-40) FCC catalyst. From the photomicrographs, the particle size of the RE-USY (Davison GO-40) FCC catalyst was found to be in the range of 30-40 μm.

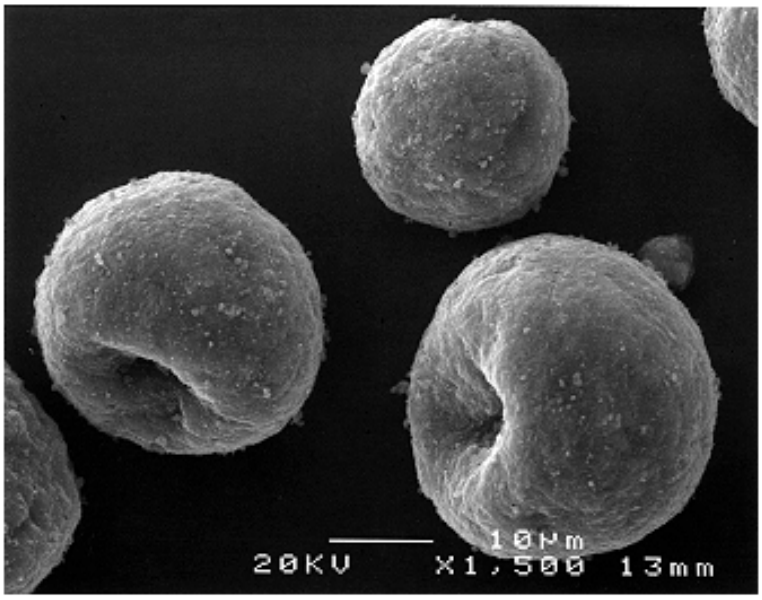

(× 1500)

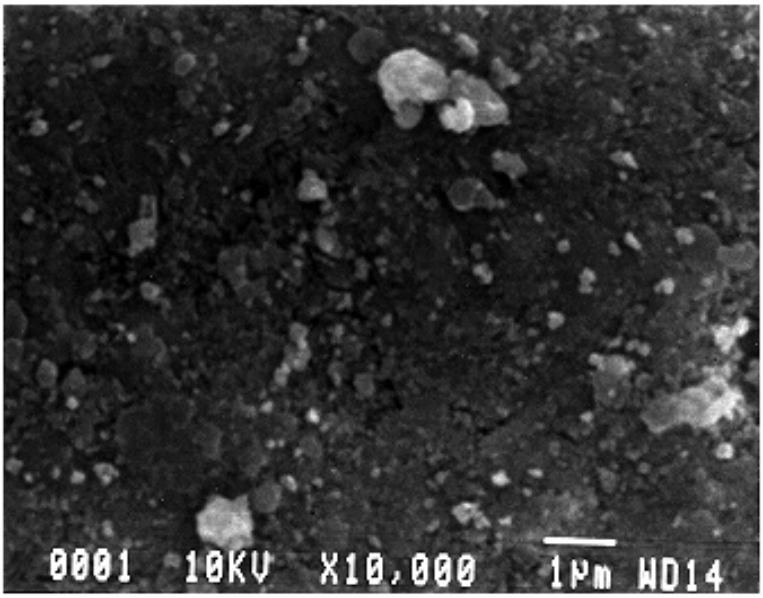

(× 10,000)

Figure 6. Scanning Electron Photomicrographs of fresh RE-USY (Davison GO-40) FCC Catalyst

4.2 Fluidized Bed Steamer-Reactor

The fluidized bed steamer-reactor used in this study was first built by Gardner (11). In the prior study of Gardner, the fluidized bed steamer-reactor was used to investigate the irreversible deactivation kinetics of H-USY (Davison Octacat) and H-ZSM-5 FCC catalysts. In this study, the work has been extended to a FCC catalyst (Davison GO-40) containing rare-earth exchanged ultra-stable Y-zeolite (RE-USY) using Gardner's test apparatus. Only the HPLC pump has been replaced with a peristaltic pump (Cole Parmer Instrument Co., Masterflex L/S Pump System model 07521-40 with pump head 07518-10). The fluidized-bed reactor (as shown in Figure 7) was fabricated from quartz glass (Quartz Scientific).

Approximately 250 samples of fluid cracking catalyst containing RE-USY zeolite (Davison GO-40) have been processed, following these procedures:

- The steamer-reactor was cleaned, in-situ, by flushing the walls of the quartz reactor with deionized water and low pressure air.
- The steamer-reactor was heated up by a single-zone furnace (Industrial Automated Systems). Temperature was read through a thermocouple placed in the reaction zone of the steamer-reactor and was controlled by an Eurotherm Programmer/Controller type 211, Mk2.
- Deionized water was supplied from a storage tank to a peristaltic pump (Cole Parmer Instrument Co., Masterflex L/S Pump System model 07521-40 with pump head 07518-10) which pumped water to the pre-heater, set at 450 °C, generating steam.
- Air was introduced and mixed with steam in the pre-heater. Air flow rate was controlled by a mass flow controller (Brooks model 5850C)

- The mixture of air and steam then traveled through heated lines to a preheating zone of the furnace which was 15 inches long, 0.25 inch diameter quartz tubing preceding the fluidized bed zone of the steamer-reactor.
- The total gas mixture flow rate was kept constant at 0.028 gram-mole/minute for all runs.
- The steam parital pressure was controlled by adjusting the flow rate of deionized water supplied to the peristaltic pump and the air flow rate.
- Samples of approximately 15 grams each were introduced into the steamer- reactor with dry air as the fluidizing gas once the desired temperature had been reached. Loading time was approximately 2 miniutes.
- The catalyst approached thermal equilibrium with fluidizing air within approximately 60 seconds. Once equilibrium had established, the desired steam partial pressure was introduced and the clock was started.
- Once timing was finished, the steam was switched off and the catalyst was dried in dry air for 30 seconds. This step was necessary to prevent clogging of catalyst in the exit valve.
- All catalyst samples were run at the temperature 600, 650, 700, 750 and 800 °C with the steam partial pressure 0, 0.2, 0.4, 0.6, 0.8 and 1.0 atmosphere for 1, 3, 6, 12 and 24 hours.

The flow diagram of the steamer-reactor process is shown in Figure 8.

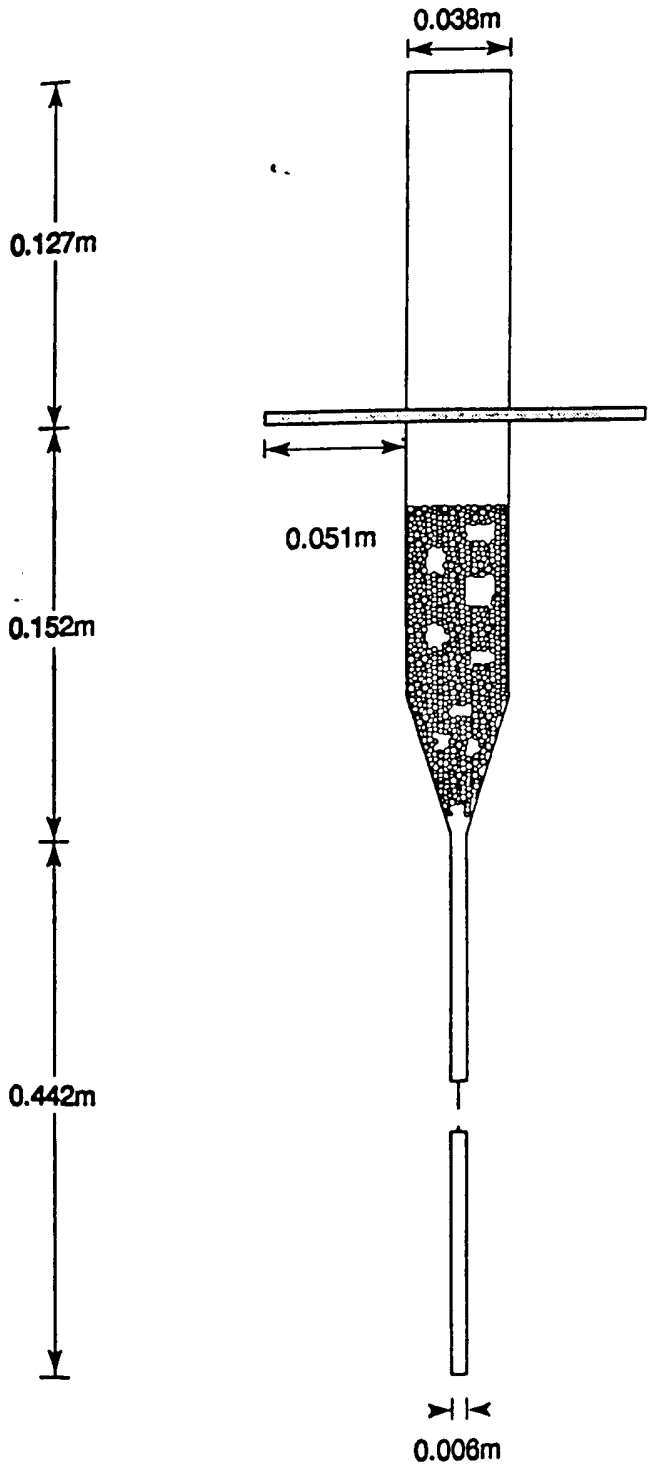

Figure 7. Fluidized Bed Steamer-Reactor (11).

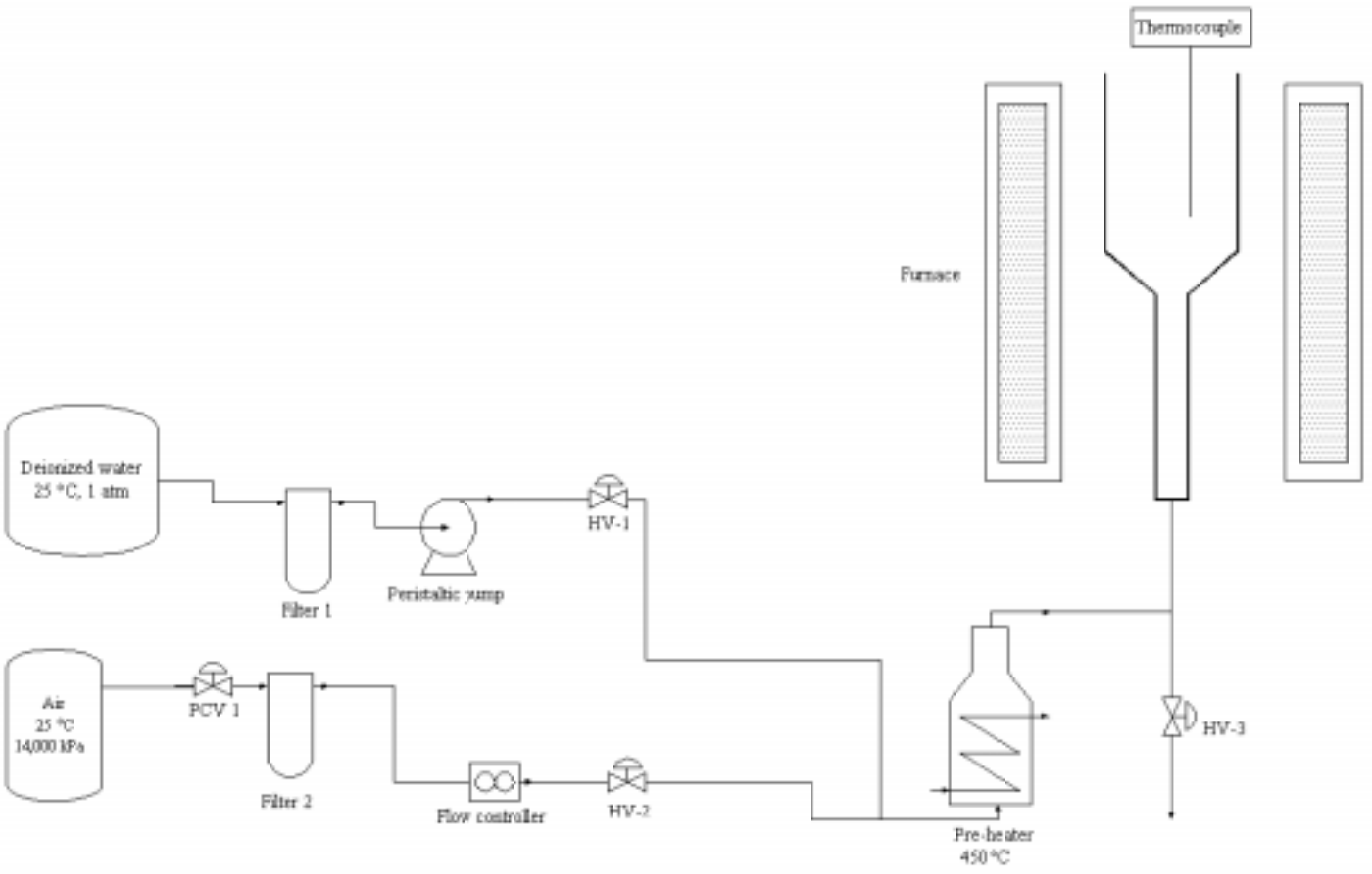

Figure 8. Flow Diagram of Fluidized Bed Steamer-Reactor.

4.3 Analytical

4.3.1 Catalyst Surface Area

The total surface area and the matrix surface area of the catalyst were measured using the nitrogen BET and t-plot surface area method described in ASTM D3363-92 “standard test method for surface area of catalysts” and ASTM D4365-85 (re-approved 1994) “Standard test method for determining zeolite area of catalysts”, respectively. The zeolite surface area was determined by subtracting the matrix surface area (t-plot) from the total surface area of the catalyst (BET).

The sorption apparatus was a Coulter OMNISORP 360. The pressure range was 0-450 Torr. The RE-USY catalyst samples were run with approximately 0.5 gram while that in the previous work of Gardner, H-USY catalyst samples were run to 350 Torr; either 0.2 or 0.5 gram catalyst. Larger sample gives more representative value; higher pressure measurement gives better t-plot.

4.3.2 Calculation of BET and t-Plot.

The procedure to calculate the total surface area (BET) and matrix surface area (t-Plot) of the catalyst is based on the Coulter Omnisorp Manual (44), Coulter Corparation, Haileah, Florida. The linear BET equation is given by:

$$\frac{P}{V(P_0-P)} = \frac{1}{V_mC} + \frac{C-1}{V_mC} \times \frac{P}{P_0}$$

Where

V_m = Volume of the monolayer

V = Volume adsorbed

P = Sample pressure

P_0 = Saturation vapor pressure

Plotting of $P/V(P_0-P)$ against P/P_0 gives a straight line having a slope $(C-1)/V_mC$ and an intercept $1/V_mC$. The BET surface area is then calculated using the following equation:

$$SA = V_m \times N \times A_m$$

Where

SA = Surface area of the sample

V_m = Volume of adsorbed monolayer

N = Avogadro's number

A_m = Cross-sectional area of the adsorbate molecule

For nitrogen, a value of 16.2 A^2 for A_m is used as the default value, and after applying the appropriate conversion factors, the equation above is simplified to:

$$SA = 4.35 \times V_m \ [M^2/g]$$

The relative pressure range of 0.001 to 0.1 was chosen for the BET calculation. The negative intercept, C-value and the correlation coefficient are the indicators whether a better relative pressure range could have been chosen.

The T-plot analysis method was developed by Lippens and deBoer (44) as a way to differentiate between the adsorption mechanism in micropores (pores with radii smaller than 10A). The method consists of plotting the adsorption isotherm in terms of the volume of gas adsorbed vs the statistical film thickness, "T". The statistical film thickness of the adsorbed gas is the thickness of the adsorbed gas on the walls of the pores. It is believed that adsorption in micropores occurs by pore filling or immediate capillary condensation. The adsorbate film

thickness calculation used for the T-plot calculation and graph is derived from the Harkins and Jura adsorption (44) equation and standard isotherm data.

$$t = [13.99/(\log P_0/P + 0.034)]^{1/2}$$

The above equation provides good results, when used over a thickness range of t = 0.35 to 0.6 nm., for this is effectively the molecular diameter of the nitrogen molecule.

According to Sing (41), when T-plot is presented over a wide thickness range, say from 1-10 A, two linear regions should be obtained. The first linear region represents both micropore filling and surface coverage of larger pores. The second linear region gives the layer-by-layer adsorption taking place in meso and macropores, but not in micropores. From the slopes and intercepts of these two linear regions, the following informations can be obtained. Micropore volume is obtained by extrapolating the second linear region to the y-axis. The y-axis intercept mutiplied by the ratio of the gas and liquid densities of the adsorbate (.00156 for nitrogen) will provide the micropore volume in cc per gram of solid. Surface area of meso and macropores is obtained from the slope of the second linear region once it is multiplied by 15.47 in order to convert to the appropriate units of square meters per gram of solid.

4.3.2 Scanning Electron Microscopy (SEM)

For scanning electron microscopy measurements the fresh and steamed RE-USY (Davison GO-40) FCC catalyst particles were scattered on double-side carbon tape, then sputter coated with gold/palladium or platinum (approximately 20 nm. thick). The images were obtained on a JEOL 6400 scanning electron microscope.

Hydrothermal stability of the RE-USY (Davison GO-40) FCC catalyst was characterized based on selected surface area and SEM data.

5.0 RESULTS AND DISCUSSION

This chapter presents and discusses the results obtained from the steam aging of RE-USY (Davison GO-40) FCC catalyst samples. Changes in zeolite surface area as a function of time, temperature and steam partial pressure were fitted into a structural kinetic model developed earlier by Gardner(11). The kinetic parameters: K_s, the apparent global zeolite hydrothermal stability rate constant, and n_s, a constant which was determined to be a function of steam partial pressure were determined and compared with those of the H-USY (Davison Octacat) catalyst.

The RE-USY (Davison GO-40) FCC catalyst samples, which were steam aged at the temperature range 600-800 °C and 0 -1 steam partial pressure in the steamer-reactor fluidized bed test apparatus, were analyzed for zeolite and matrix surface area reduction using the nitrogen BET and t-plot surface area methods. Figures 9, 10 and 11 show the nitrogen adsorption isotherm, BET surface area and t-plot surface area of the1 hour steamed RE-USY (Davison GO-40) FCC catalyst at 700 °C and 0.6 atm steam partial pressure, respectively. From the nitrogen adsorption data, adsorption isotherm for both fresh and steam-aged catalysts were suggested to be a combination of type I (microporous solid) and type IV (mesoporous solid). The FCC catalyst is a complex composite with two main components: zeolite and matrix. The zeolite portion is characterized by micropores. Micropores filling at a low-relative pressure range will result in type I isotherm. And when the relative pressure reaches a value that a capillary condensation of mesopores occurs, a type IV isotherm will result.

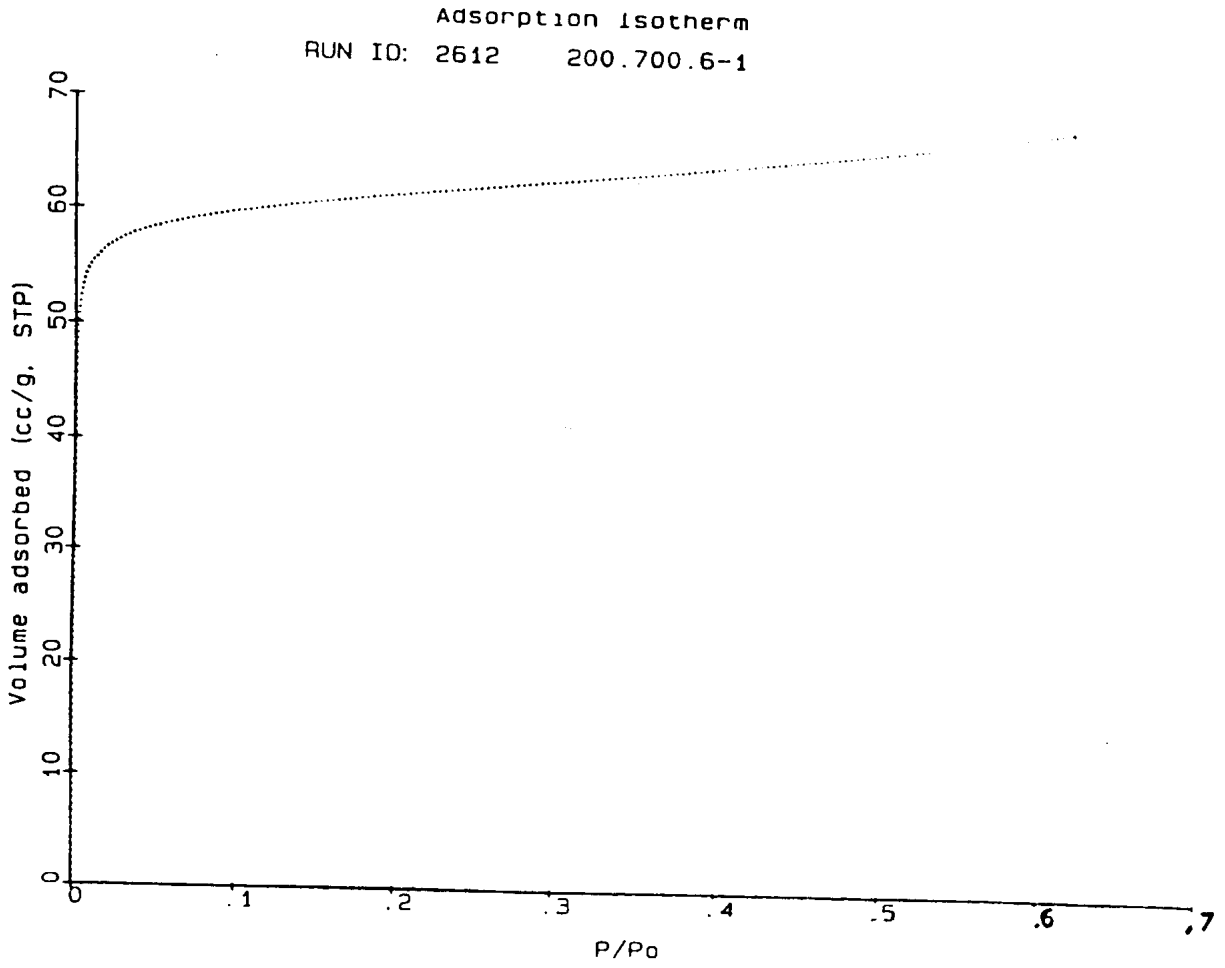

Figure 9. Nitrogen adsorption isotherm of 1 hr. steam aged RE-USY at 700 °C and 0.6 atm steam partial pressure.

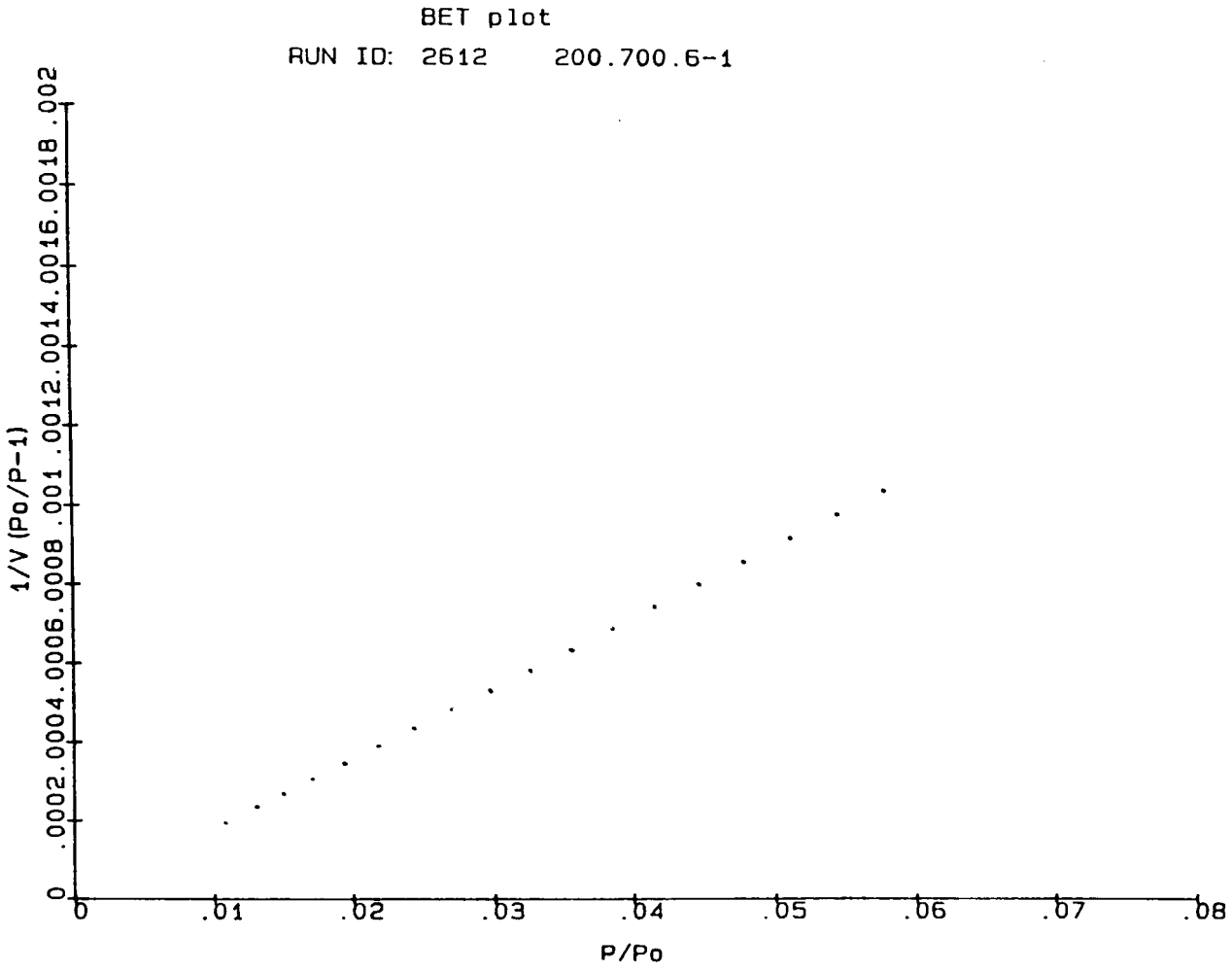

Figure 10. BET plot surface areaof steam aged RE-USY at 700 °C and 0.6 atm steam partial pressure for 1 hour.

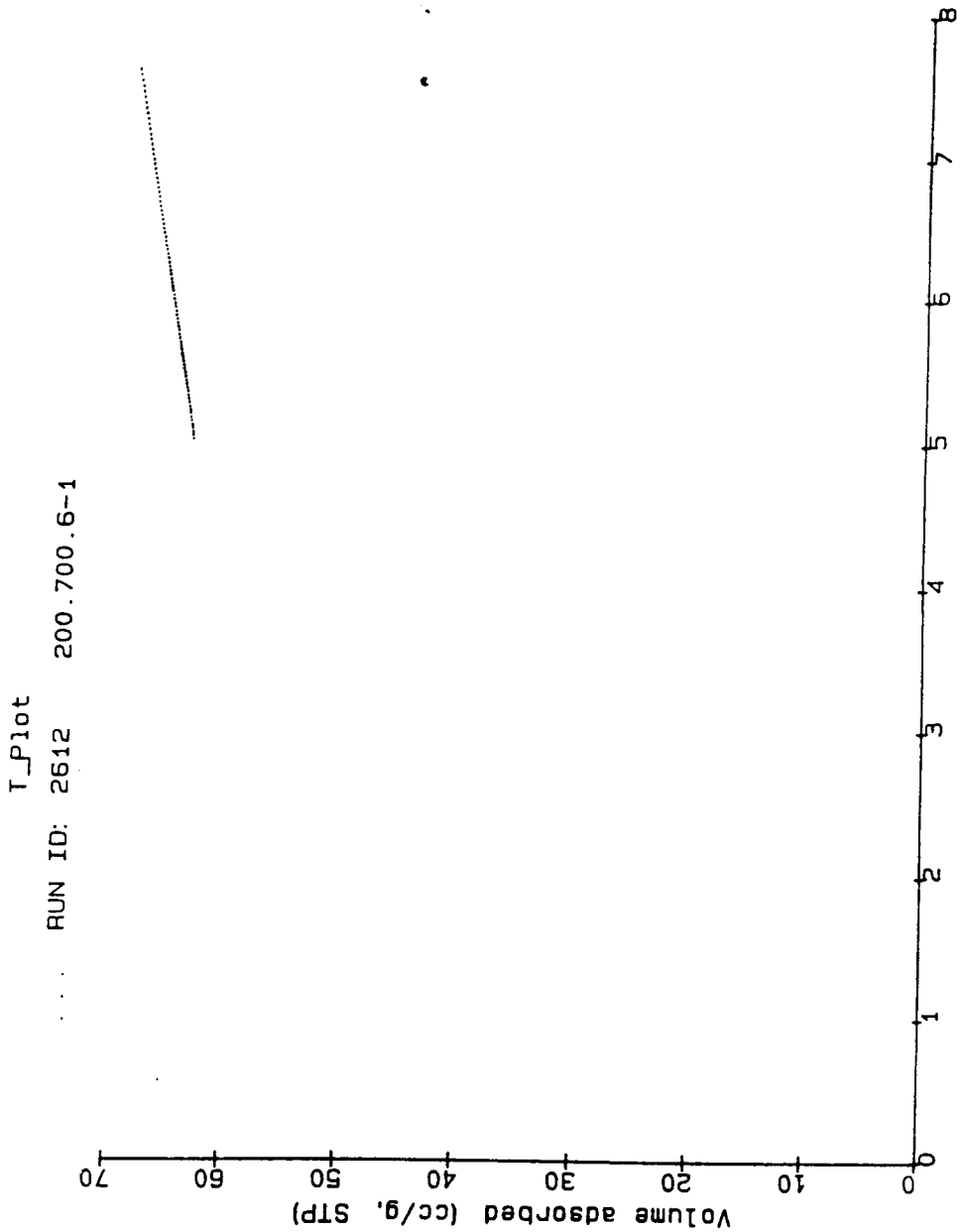

Figure 11. T-plot surface areaof steam aged RE-USY at 700 °C and 0.6 atm steam partial pressure for 1 hour.

The reduction of surface area of the catalysts as a function of temperature, steam partial pressure and time leads to the irreversible deactivation kinetics of the catalysts. Gardner's surface area reduction model (11) for the USY catalysts was applied to the studying of RE-USY here in order to compare their hydrothermal stability. Based on Gardner's model, observed changes in zeolite surface area were found to be proportional to the time on stream by the relationship

$$[(S_0 - S)/S_0]^{ns} \quad \alpha \quad t$$

where S_0 is the initial surface area, S is the surface area at time t, t is time on stream and n_s is a constant which was determined to be a function of steam partial pressure at a given temperature. A constant was added to make an equal proportionality. The expression then became

$$[(S_0 - S)/S_0]^{ns} \quad = \quad K_s\, t$$

K_s is an apparent global hydrothermal stability rate constant which is a function of temperature given by an Arrhenius-type relationship

$$K_s = k_{s0} \exp(-E_A/RT)$$

where E_A is an apparent activation energy for zeolite hydrothermal stability, k_0 is a pre-exponential factor, R is the gas constant and T is an absolute temperature.

The deactivation kinetics model then was written as

$$[(S_0-S)/S_0]^{ns} \quad = \quad k_{s0}\, e^{(-Ea/RT)}\, t$$

As mentioned by Gardner (11), the surface area kinetic model developed could be possibly used as a quantitative analytical tool to compare one faujasite-type FCC catalyst hydrothermal stability to another's by comparison of their kinetic parameters, K_s and n_s at the same conditions. Figures 12 -16 are plots of the RE-USY (Davison GO-40) FCC catalyst surface area decline at 600, 650, 700, 750 and 800 °C as a function of the time on stream and steam

partial pressure. The model based prediction were shown in lines while the experimental measured values were shown as points. From the plots, the RE-USY (Davison GO-40) FCC catalyst lost surface area rapidly within the first hour when presented into a high-temperature hydrothermal environment. These changes continued at the lower rate over the next 24 hours. Equilibrium surface area values were reached after 6 hours. Large initial changes in the RE-USY zeolite surface area occurred when contacted with one atmosphere steam partial pressure within the first hour. The steam partial pressure as low as 0.2 atm also induced large initial changes in zeolite surface area of the RE-USY within the first hour. However when presented into non-steam environment in the temperature ranges 600-800 °C, the RE-USY exhibited high thermal stability. The measured total (BET) and matrix (t-plot) surface area of fresh and steam aged RE-USY (Davison GO-40) FCC catalyst are given in Appendix A. The data in the temperature range 500-550 °C did not include in the calculation of the kinetic parameters due to the occurrence of small changes and inconsistent of data.

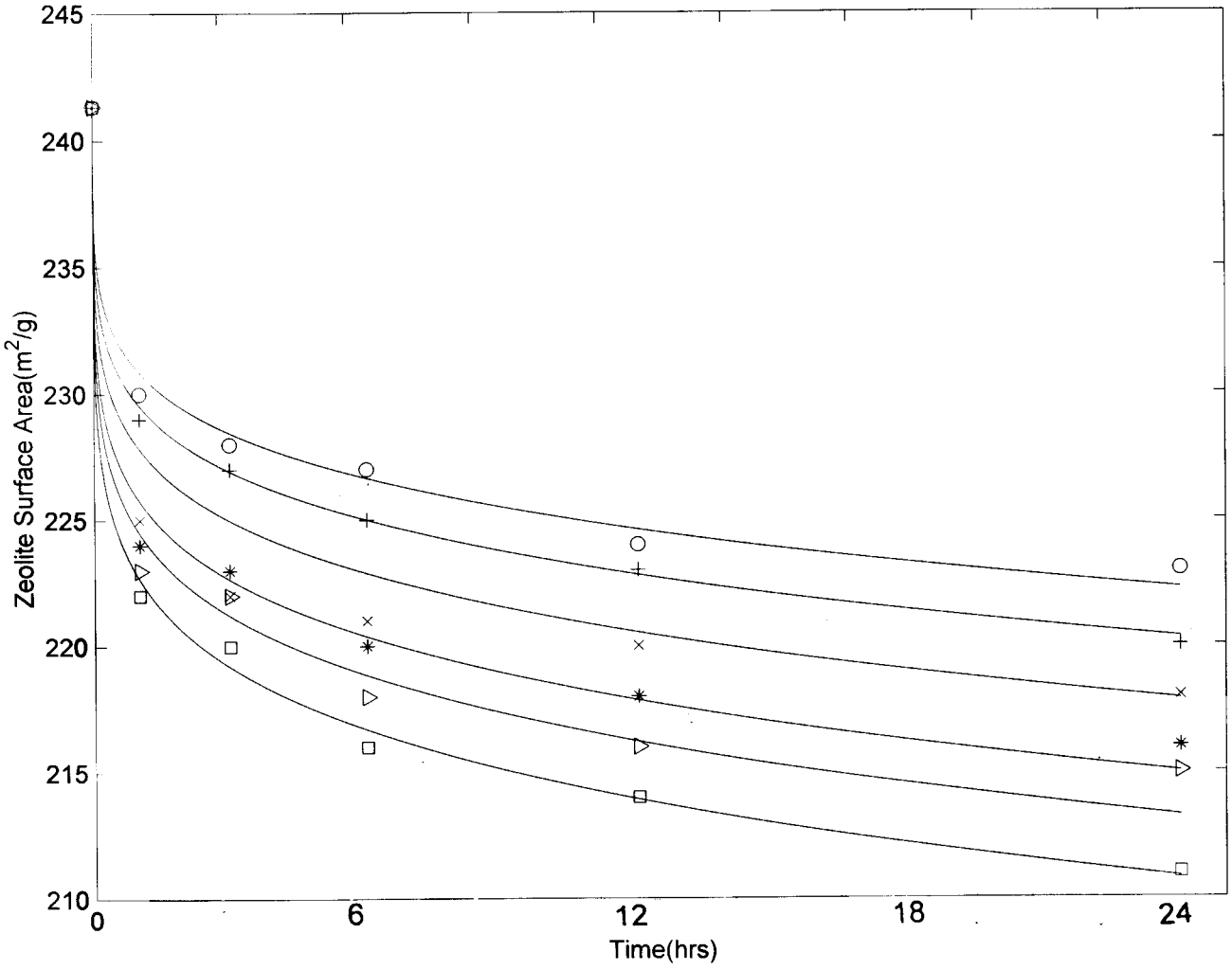

Figure 12. RE-USY zeolite surface area hydrothermal stability curve at 600 °C and various steam partial pressure as a function of time.

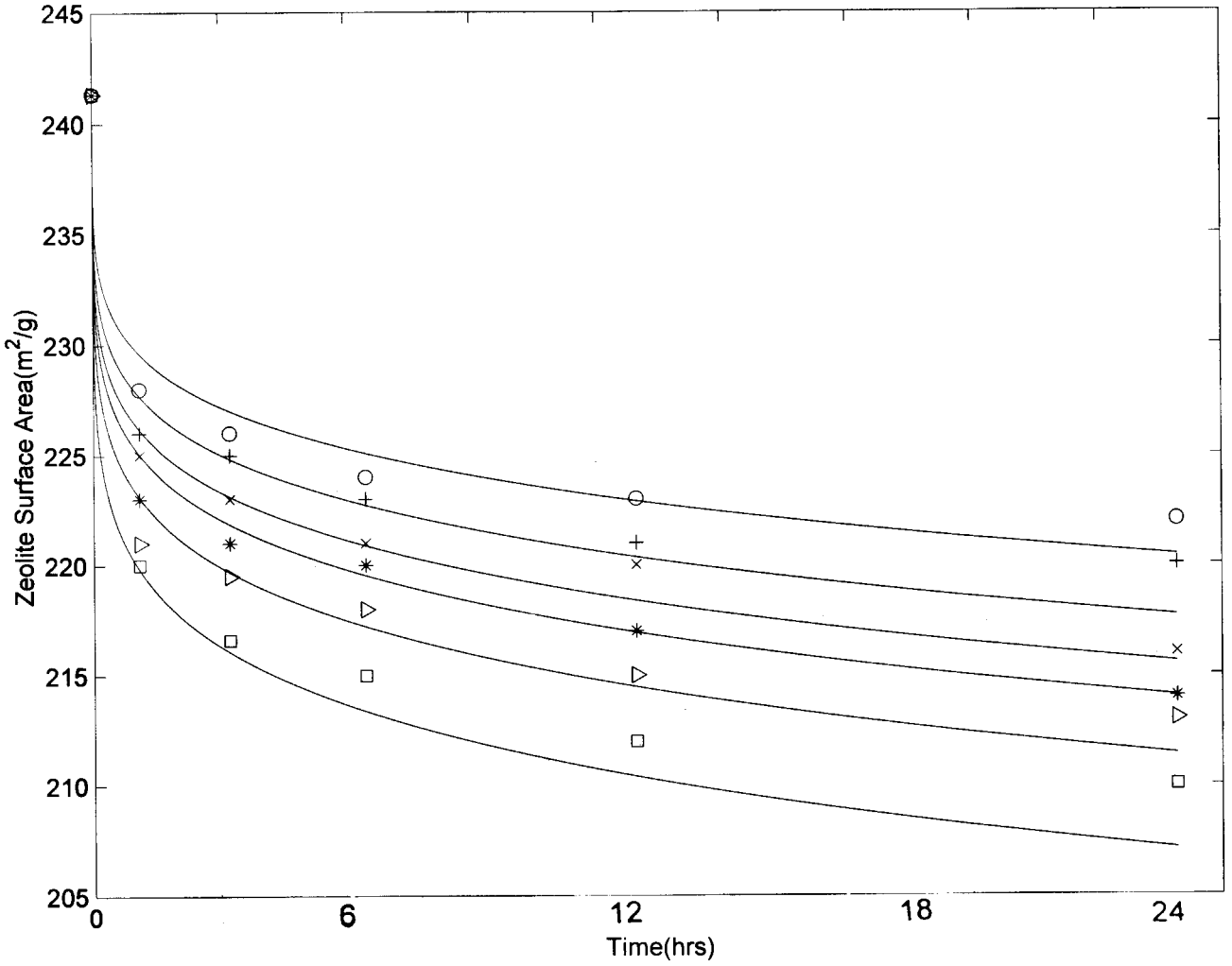

Figure 13. RE-USY zeolite surface area hydrothermal stability curve at 650 °C and various steam partial pressure as a function of time.

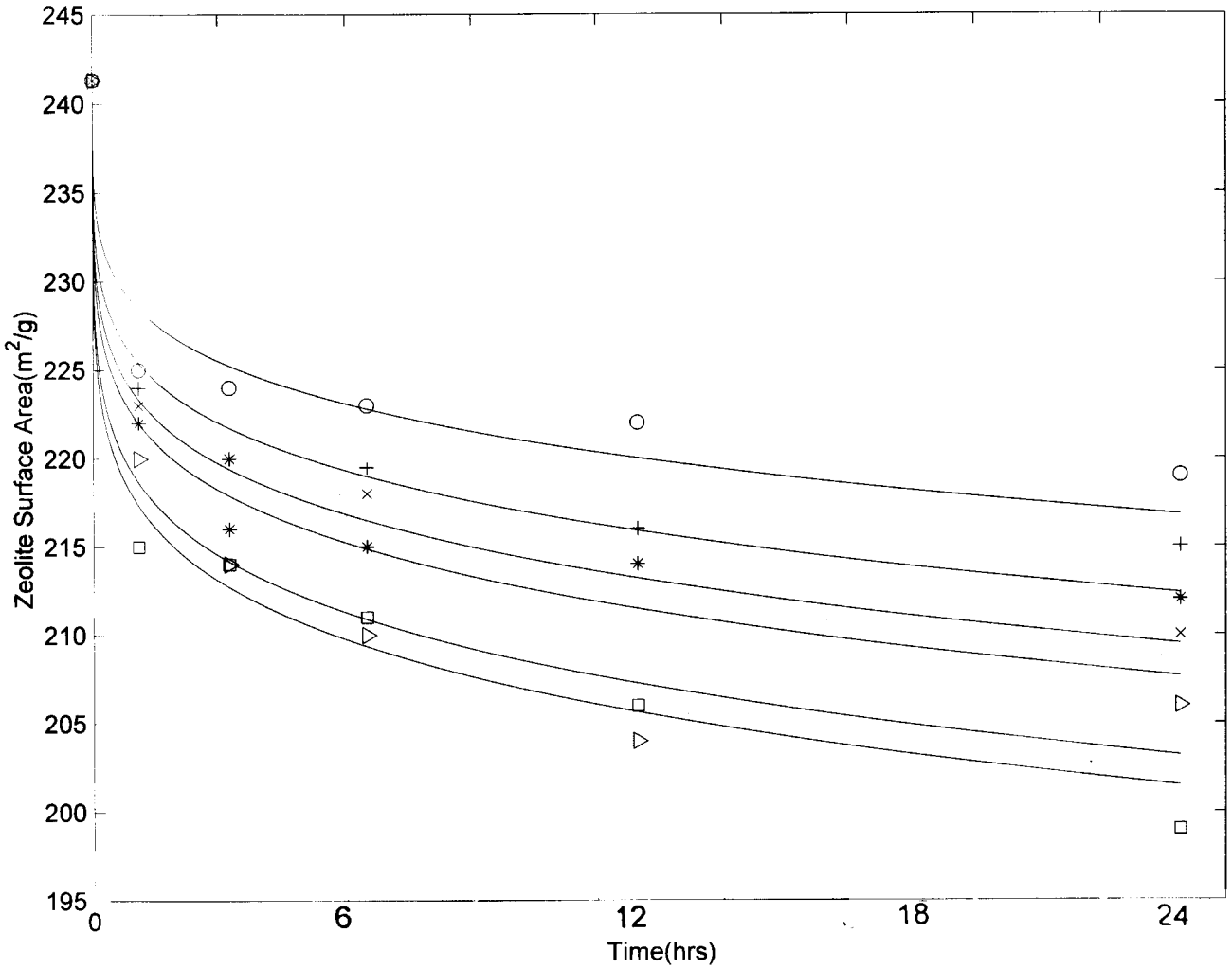

Figure 14. RE-USY zeolite surface area hydrothermal stability curve at 700 °C and various steam partial pressure as a function of time.

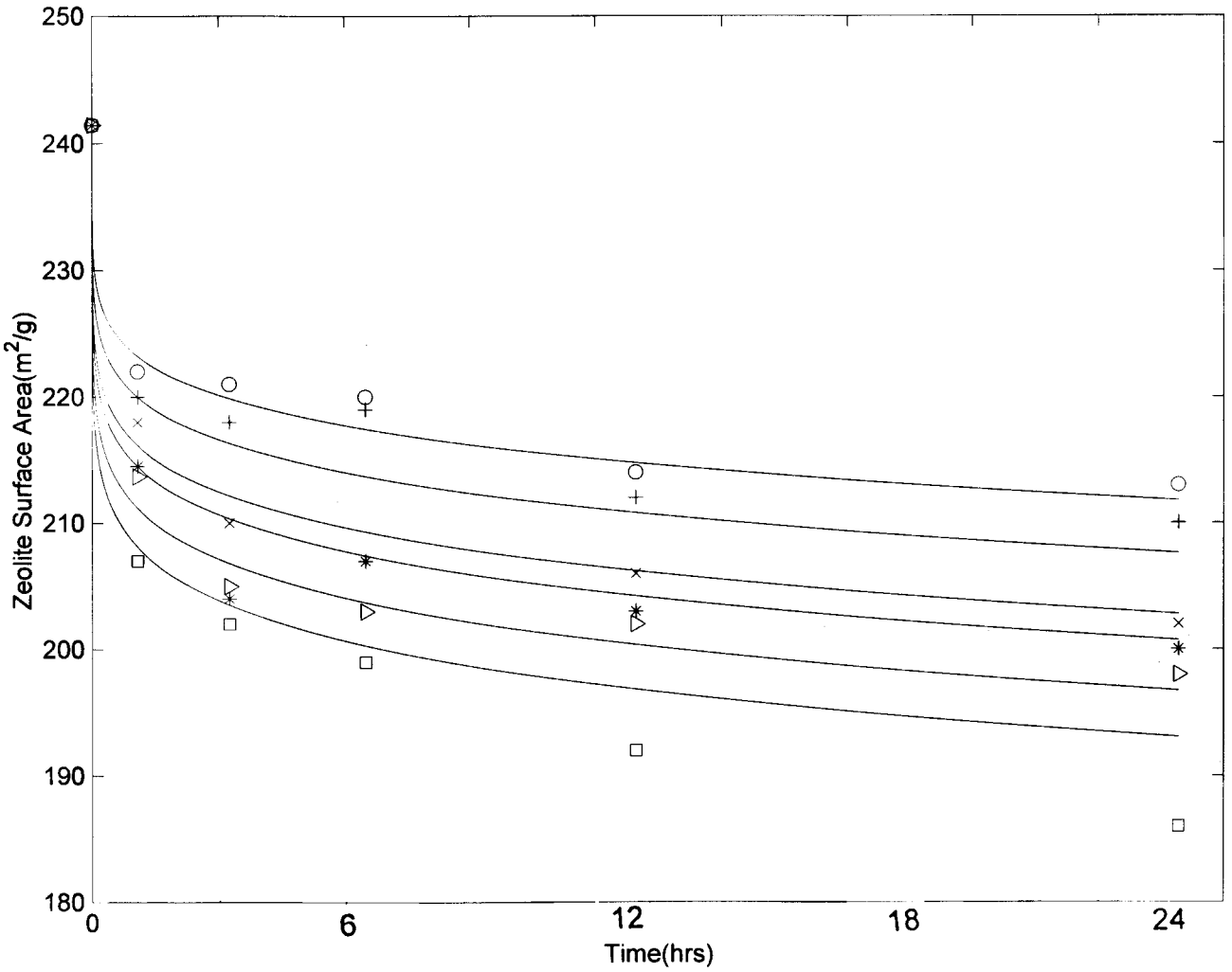

Figure 15. RE-USY zeolite surface area hydrothermal stability curve at 750 °C and various steam partial pressure as a function of time.

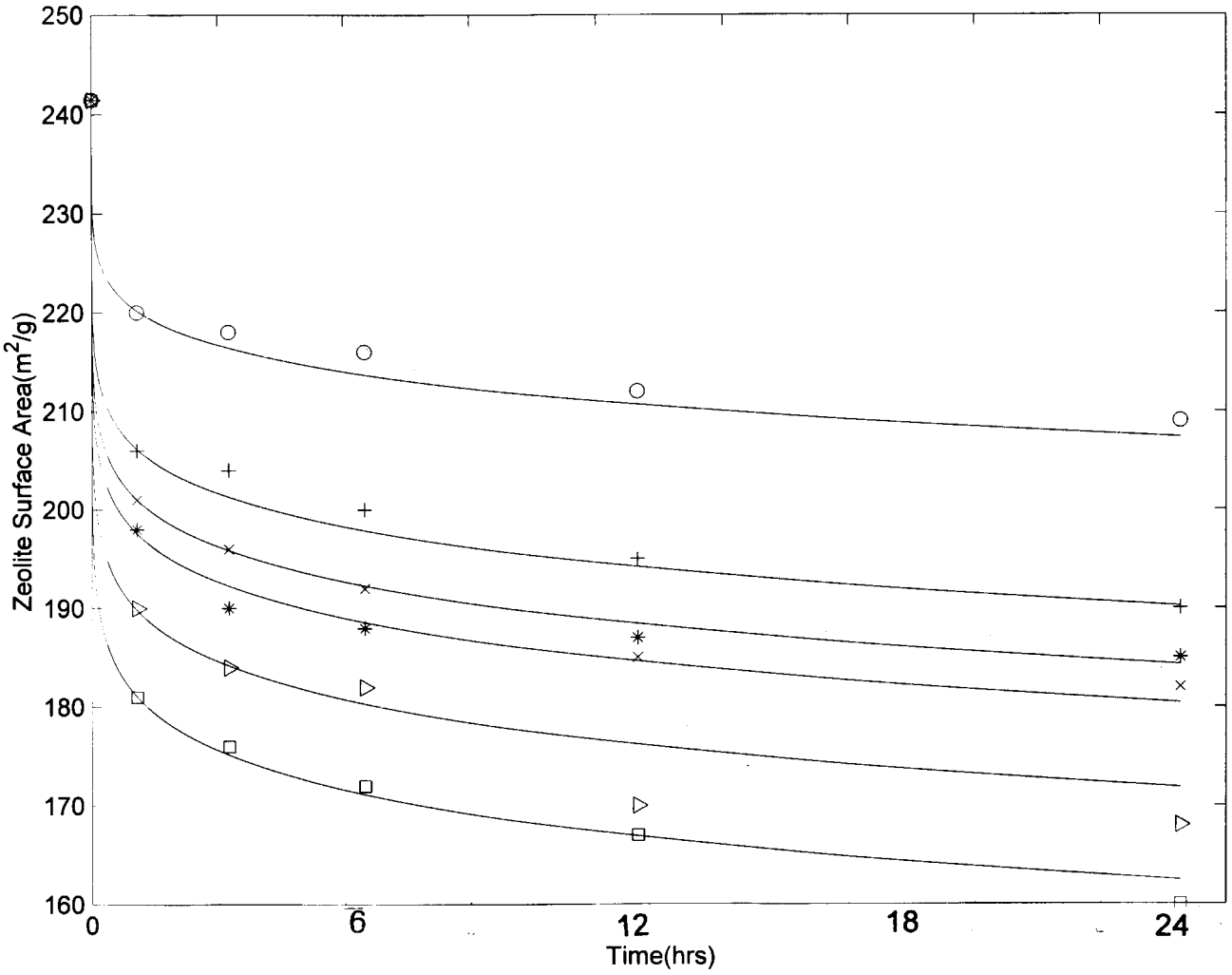

Figure 16. RE-USY zeolite surface area hydrothermal stability curve at 800 °C and various steam partial pressure as a function of time.

Data analysis was performed by the following two methods. In the first method, the apparent activation energy for zeolite hydrothermal stability (E_A) and the pre-exponential factor (k_{s0}) were assumed to be constant throughout the experimental conditions (temperature ranges from 600-800^oC, steam partial pressure 0-1 atm, and time 0-24 hours). The apparent global hydrothermal stability rate constant, K_s, is then a constant at a fixed temperature where n_s varied with the steam partial pressure. The second method, all kinetic parameters, E_A, k_{s0}, and n_s varied with temperature and steam partial pressure.

The best fit for the kinetic parameters, E_A, k_{s0}, and n_s, for the RE-USY (Davison GO-40) FCC catalyst using method 1 are given in Table 3. The calculated K_s and n_s for each condition are given in Table 4. The fit of the experimental data by the surface area kinetic model developed can be considered satisfactory, as illustrated in Figure 17. Normalized residual values (measured values - predicted values / measured values x 100) for selected points given in Table 5 shows the surface area prediction errors which were less than ten percent.

Table 3: Surface area best-fit parameters.

Temp.(°C)	E_A (J/mol)	k_{s0} , (hr^{-1})	n_s
600	94,565	28.6	$n_s = 0.5786P_{steam} + 3.2395$
650	94,565	28.6	$n_s = 0.5953P_{steam} + 3.1136$
700	94,565	28.6	$n_s = 0.8424P_{steam} + 3.2226$
750	94,565	28.6	$n_s = 1.0178P_{steam} + 3.1308$
800	94,565	28.6	$n_s = 2.0585P_{steam} + 3.2283$

Table 4: **Best fit kinetic parameters; K_s and n_s for hydrothermal aging of the RE-USY zeolite catalyst.**

Temp. (^oC)	Steam (atm)	K_s (hr^{-1})	n_s
600	0	6.28E-05	3.25
	0.2	6.28E-05	3.36
	0.4	6.28E-05	3.47
	0.6	6.28E-05	3.59
	0.8	6.28E-05	3.65
	1.0	6.28E-05	3.86
650	0	1.27E-04	3.11
	0.2	1.27E-04	3.24
	0.4	1.27E-04	3.32
	0.6	1.27E-04	3.47
	0.8	1.27E-04	3.65
	1.0	1.27E-04	3.67
700	0	2.40E-04	3.17
	0.2	2.40E-04	3.46
	0.4	2.40E-04	3.56
	0.6	2.40E-04	3.73
	0.8	2.40E-04	3.89
	1.0	2.40E-04	4.06
750	0	4.24E-04	3.13
	0.2	4.24E-04	3.33
	0.4	4.24E-04	3.58
	0.6	4.24E-04	3.74
	0.8	4.24E-04	3.82
	1.0	4.24E-04	4.23

Table 4. (cont.)

Temp. (^{o}C)	Steam (atm)	K_s (hr^{-1})	n_s
800	0	7.12E-04	3.12
	0.2	7.12E-04	3.77
	0.4	7.12E-04	4.06
	0.6	7.12E-04	4.46
	0.8	7.12E-04	4.88
	1.0	7.12E-04	5.26

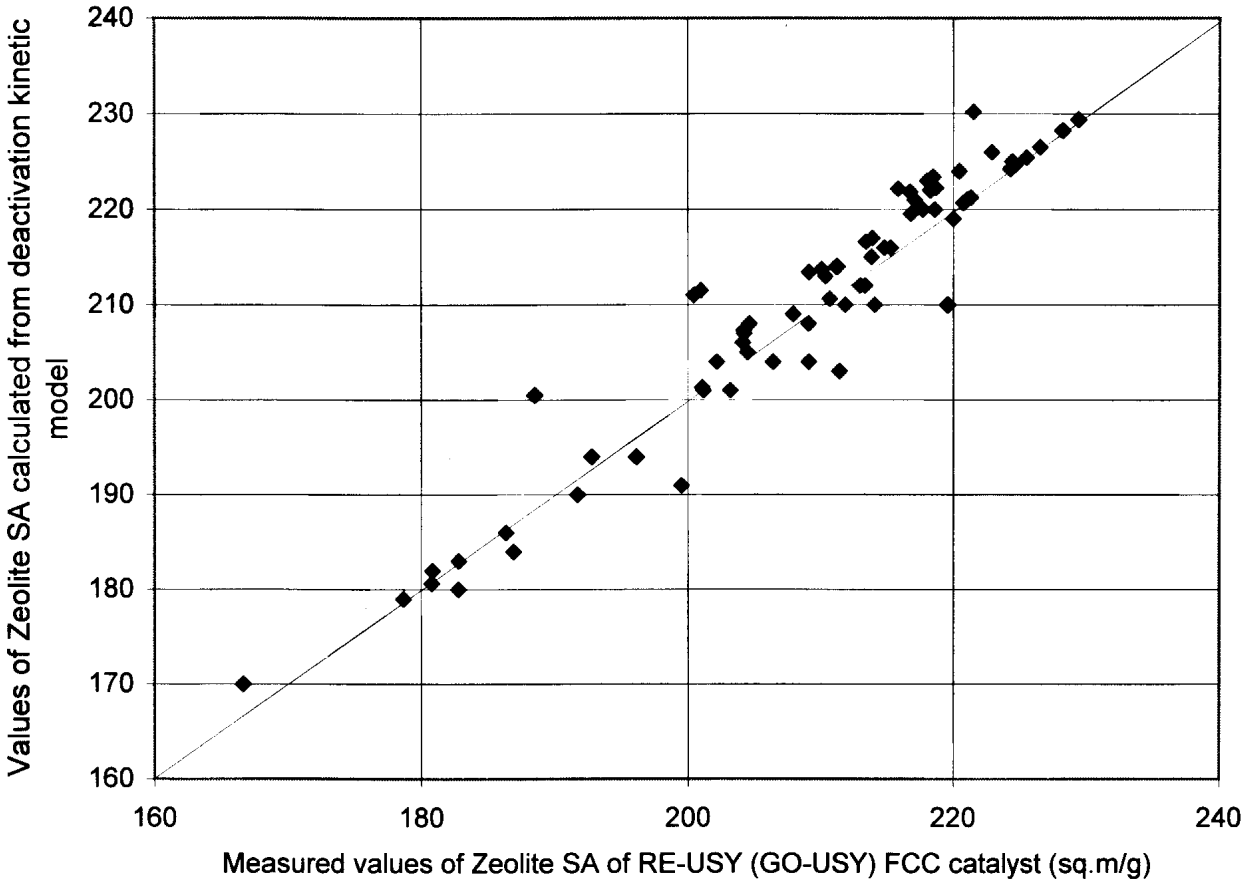

Figure 17. Adequacy of fit of the measured RE-USY zeolite surface area data to the model predicted values.

Table 5: The RE-USY zeolite surface area prediction errors (selected points)

Temp.(°C)	P_{steam}(atm)	Time(hrs)	Meas.(m^2/g)	Pred.(m^2/g)	Meas-Pred/Measx100
600	0	1	229.42	229.43	-0.002
600	0.2	3	229.25	222.91	2.76
600	0.4	6	219.55	216.81	1.25
600	0.6	24	212.96	202.17	5.06
600	0.8	6	215.00	213.86	0.53
600	1.0	12	216.76	210.4	4.65
650	0	1	228.26	228.23	0.012
650	0.2	3	225.80	220.45	2.367
650	0.4	6	223.98	213.9	4.486
650	0.6	3	221.82	216.73	2.294
650	0.8	1	221.04	221.043	-0.002
650	1.0	12	209.80	200.46	4.45
700	0	3	224.56	217.08	3.33
700	0.2	1	219.98	220	-0.009
700	0.4	6	219.52	206.3	6.02
700	0.6	24	213.57	201.07	5.85
700	0.8	3	213.67	207.11	3.07
700	1.0	12	205.54	201.06	2.18

Table 5. (cont.)

Temp.(°C)	P_{steam}(atm)	Time(hrs)	Meas.(m^2/g)	Pred.(m^2/g)	Meas-Pred/Measx100
750	0	3	222.59	221.52	3.76
750	0.2	1	227.45	218.26	4.04
750	0.4	6	207.31	204.2	1.50
750	0.6	12	192.78	182.84	5.16
750	0.8	3	197.9	191.8	3.10
750	1.0	3	179.802	180.02	-0.22
800	0	1	223.23	218.050	2.31
800	0.2	24	190.8	189.59	0.634
800	0.4	6	189.03	180.67	0.553
800	0.6	3	188.83	180.84	4.23
800	0.8	12	169.36	160.64	5.1487
800	1.0	1	180.65	180.79	-0.078

Comparison of the kinetic parameters, K_s and n_s, for zeolite surface area reduction of the RE-USY (Davison GO-40) and H-USY (Davison Octacat) FCC catalysts at one atmosphere steam partial pressure and temperature 650-800^oC are shown in Table 6.

Table 6: Comparison of the kinetic parameters at one atmosphere steam partial pressure and temperature ranges from 650-800^oC.

	RE-USY		H-USY	
	K_s (hr^{-1})	n_s	K_s (hr^{-1})	n_s
650 ^oC	$1.27x10^{-4}$	3.67	$2.31x10^{-3}$	7.67
700 ^oC	$2.40x10^{-4}$	4.06	$4.69x10^{-3}$	7.25
750 ^oC	$4.24x10^{-4}$	4.23	$8.89x10^{-3}$	7.33
800 ^oC	$7.12x10^{-4}$	5.26	$1.58x10^{-2}$	8.54

The total surface area (BET), matrix surface area (t-plot) and zeolite surface area of fresh and steam aged H-USY (Davison Octacat) FCC catalyst are given in Appendix B. The best fit values for n_s, k_{s0}, and E_A for the H-USY (Davison Octacat) FCC catalyst calculated by Gardner(11) using method 1 are given in Appendix C. The K_s and n_s values at each condition for the H-USY were calculated and given in Appendix D. The calculation procedure for K_{s0}, n_s, E_A and k_{s0} is described in Appendix E.

In Method 2, the three kinetic parameters were re-calculated follow the same procedure as described in Method 1 only that the apparent activation energy (E_A) and the pre-exponential factor (k_{s0}) were varied with temperature and steam partial pressure. The results are shown in Table 7.

Table 7: Values of E_A and k_{s0} when varied with temperature and steam partial pressure.

Temp.(^oC)	P_{steam} (atm)	$K_s(hr^{-1})$	K_s (avg.)	E_A(J/mol)	k_{s0} (hr^{-1})
600	0	6.55E-05			29.83
	0.2	5.90E-05			26.87
	0.4	2.19E-05	6.23E-05		9.97
	0.6	7.40E-05			33.70
	0.8	9.31E-05			42.40
	1.0	6.03E-05			27.46
				96,501.6	
650	0	9.01E-05			20.26
	0.2	7.09E-05			15.94
	0.4	5.13E-05	1.29E-04		11.53
	0.6	1.42E-04			31.92
	0.8	1.28E-04			28.78
	1.0	2.92E-04			65.65
				92,716.03	
700	0	1.06E-04			12.65
	0.2	2.91E-04			34.73
	0.4	1.74E-04	2.40E-04		20.77
	0.6	2.17E-04			25.90
	0.8	2.64E-04			31.51
	1.0	3.88E-04			46.31
				95,547.05	
750	0	2.42E-04			16.31
	0.2	5.50E-04			37.06
	0.4	5.91E-04	4.23E-04		39.83
	0.6	1.68E-04			11.32
	0.8	7.43E-04			50.07
	1.0	2.44E-04			16.44
				93,495.48	
800	0	6.70E-04			26.90
	0.2	8.31E-04			33.36
	0.4	7.23E-04	7.06E-04		29.03
	0.6	6.78E-04			27.22
	0.8	6.09E-04			24.45
	1.0	7.25E-04			29.11
				Avg. E_A = 94,565	Avg. k_{s0}=28.576

Several interesting points were noted while performing data analysis using method 2. The apparent global hydrothermal stability rate constant (K_s) values did not show much variation with the steam partial pressure in the same temperature. K_s should be constant at a fixed temperature. The activation energy, E_A, is also considered constant throughout the experimental temperature range (600-800 ^oC). Only the pre-exponential factor, k_{s0}, shows large variations with temperature and steam partial pressure. No trend was observed. The variation intervals shown in Table 8 indicated corresponding to the standard errors determined for the different kinetic parameters.

Table 8. The variation intervals of the kinetic parameters.

	Method 1	Method 2
E_A (J/mol)	94,565	94,565 +/- 2,000
k_{s0} (hr^{-1})	28.6	28.576 +/- 37
N_s	Function of P_{steam}	Function of P_{steam} +/- 0.02

However, Method 2 for calculation of the kinetic parameters does not appear to be satisfactory due to the inconsistent values of k_{s0}.

Figure 18 shows the RE-USY t-plot surface area at one atmosphere steam partial pressure and various temperatures as a function of time. Unlike the deep and complex modification of the zeolite framework, the decrease in surface area of the matrix is due to sintering of the particles, increasing their size. The pore volume of the silica-alumina remains more or less constant (1). The lack of an observed increase in t-plot surface area with steam aging severity suggested that the destroyed zeolite material was not forming mesoporosity to any appreciable extent under the investigation conditions.

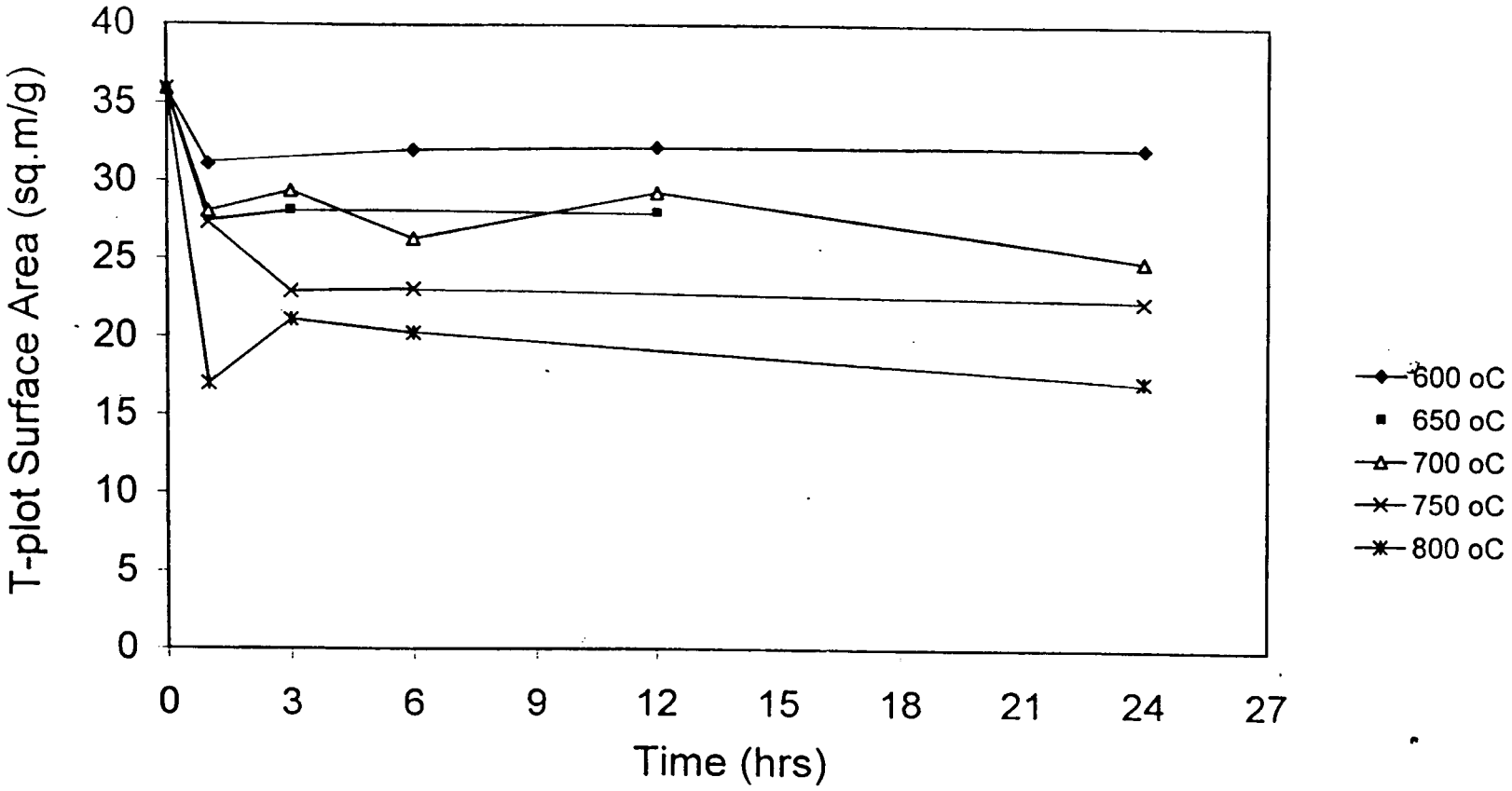

Figure 18. RE-USY t-plot surface area at one atm steam partial pressure and various temperature as a function of time.

Figures 19-23 show the RE-USY t-plot surface area hydrothermal stability at 600, 650, 700, 750 and 800 °C and various steam partial pressure as a function of time. The fresh and steam aged RE-USY (Davison GO-40) FCC catalyst surface morphology were apparent from the scanning electron photomicrographs shown in Figures 24. The surface morphology of the fresh RE-USY (Davison GO-40) FCC catalyst was characterized as being made up of agglomerated spheroids. The agglomerated spheroids in the fresh catalysts became noticeable sintered and flatter after the catalysts were steam aged. However, the smooth external surface may have resulted from particles rubbing against each other in the fluidized bed.

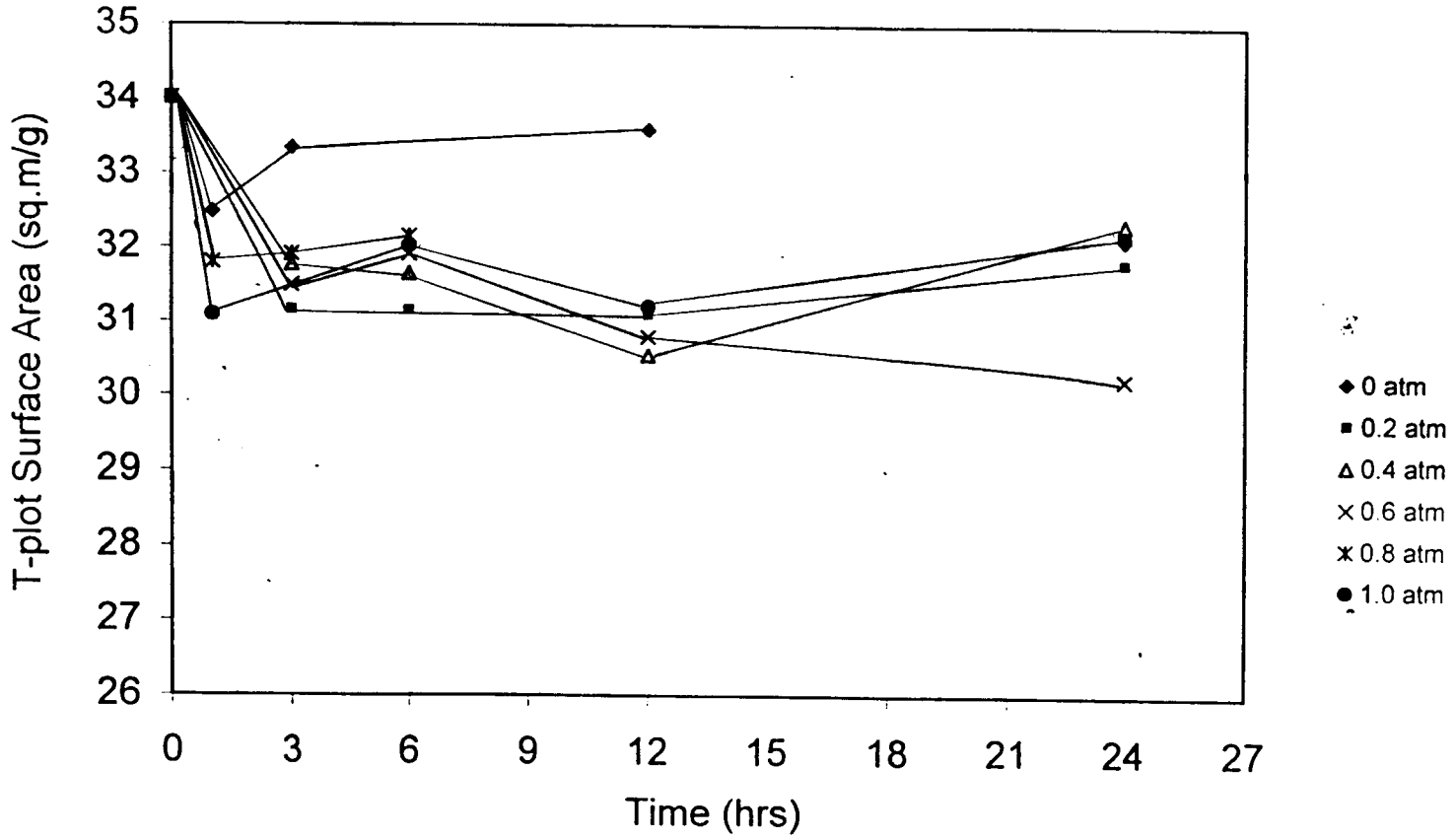

Figure 19. RE-USY t-plot surface area hydrothermal stability at 600 °C and various steam partial pressure as a function of time.

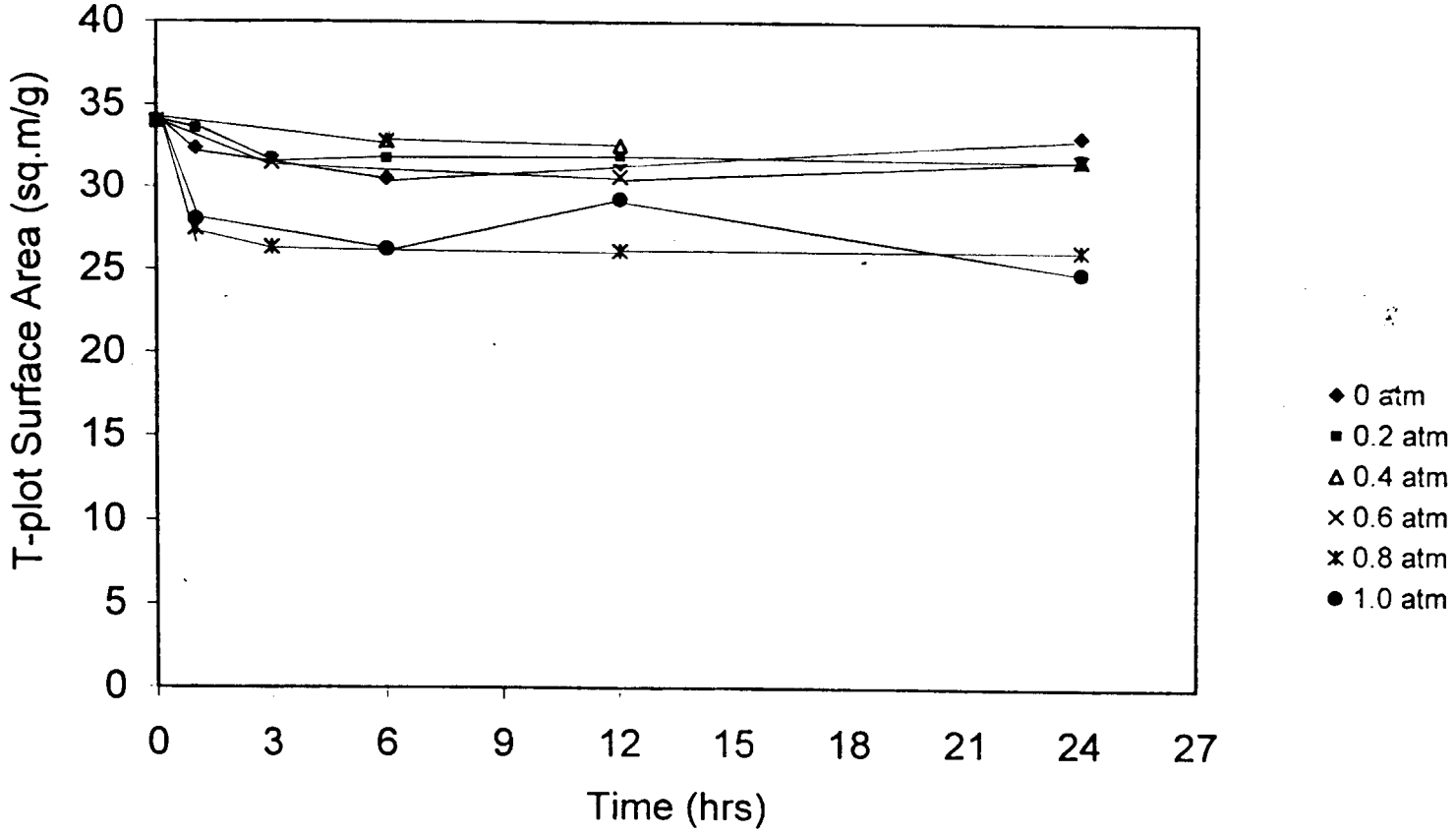

Figure 20. RE-USY t-plot surface area hydrothermal stability at 650 °C and various steam partial pressure as a function of time.

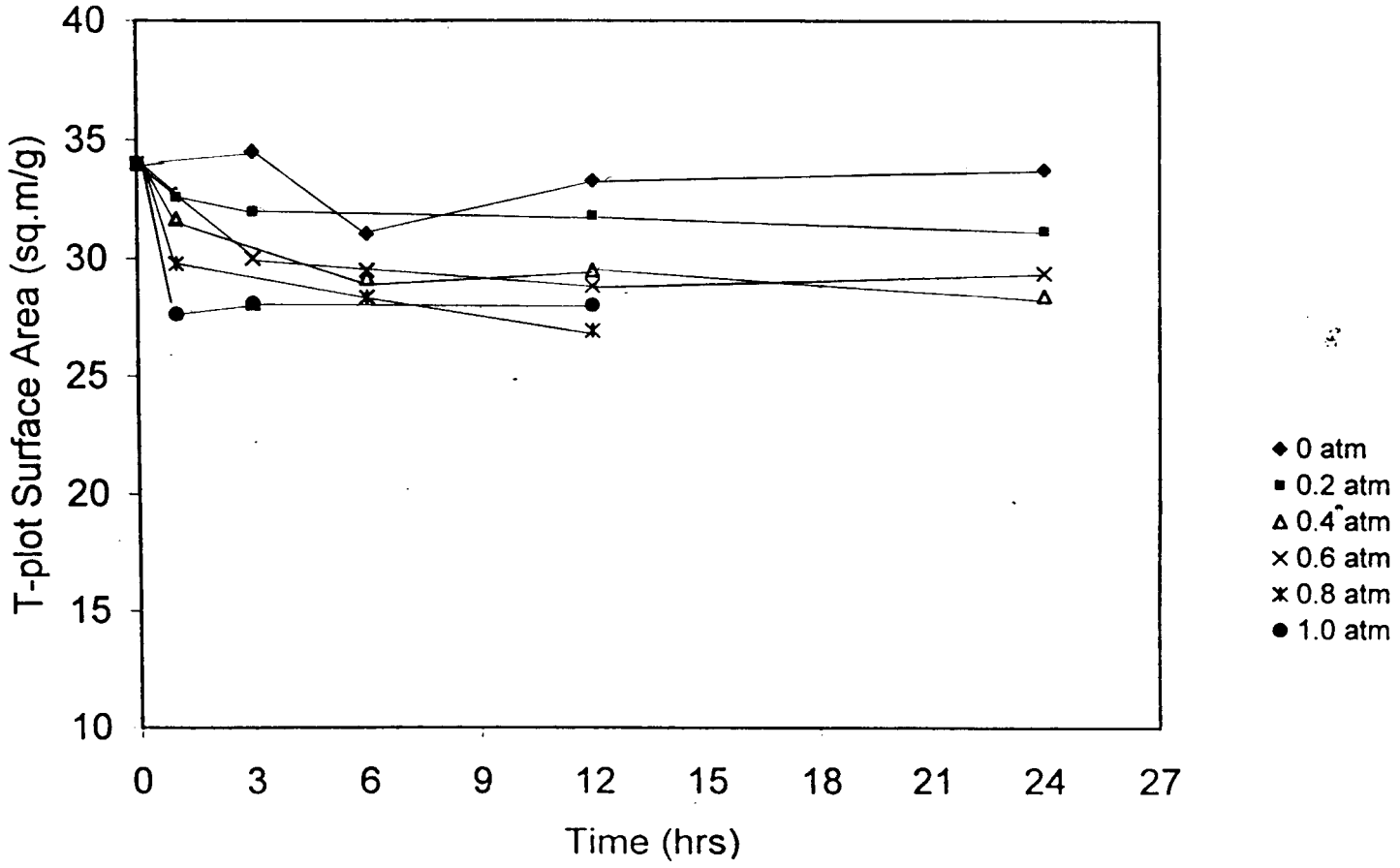

Figure 21. RE-USY t-plot surface area hydrothermal stability at 700 °C and various steam partial pressure as a function of time.

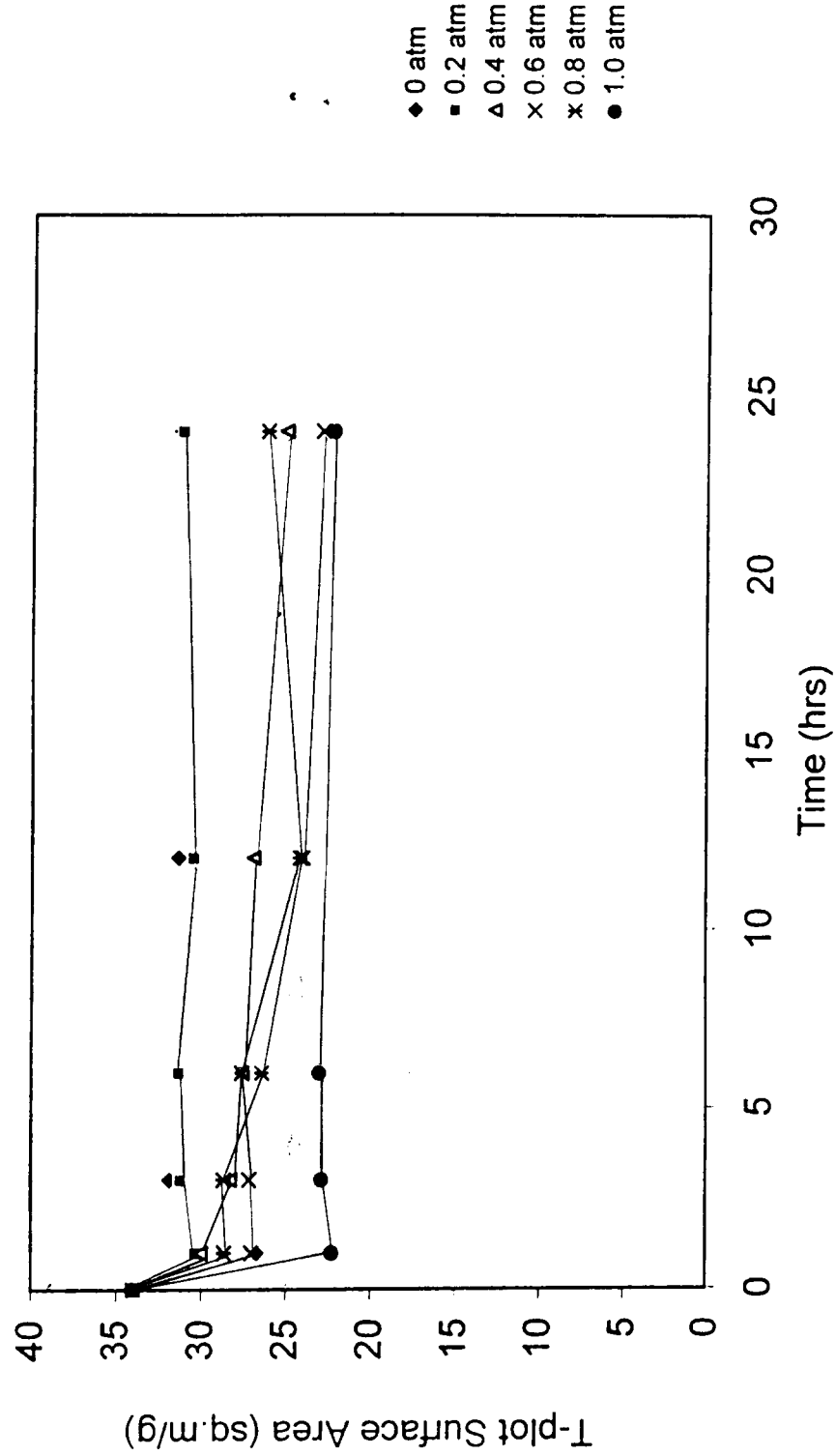

Figure 22. RE-USY t-plot surface area hydrothermal stability at 750 °C and various steam partial pressure as a function of time.

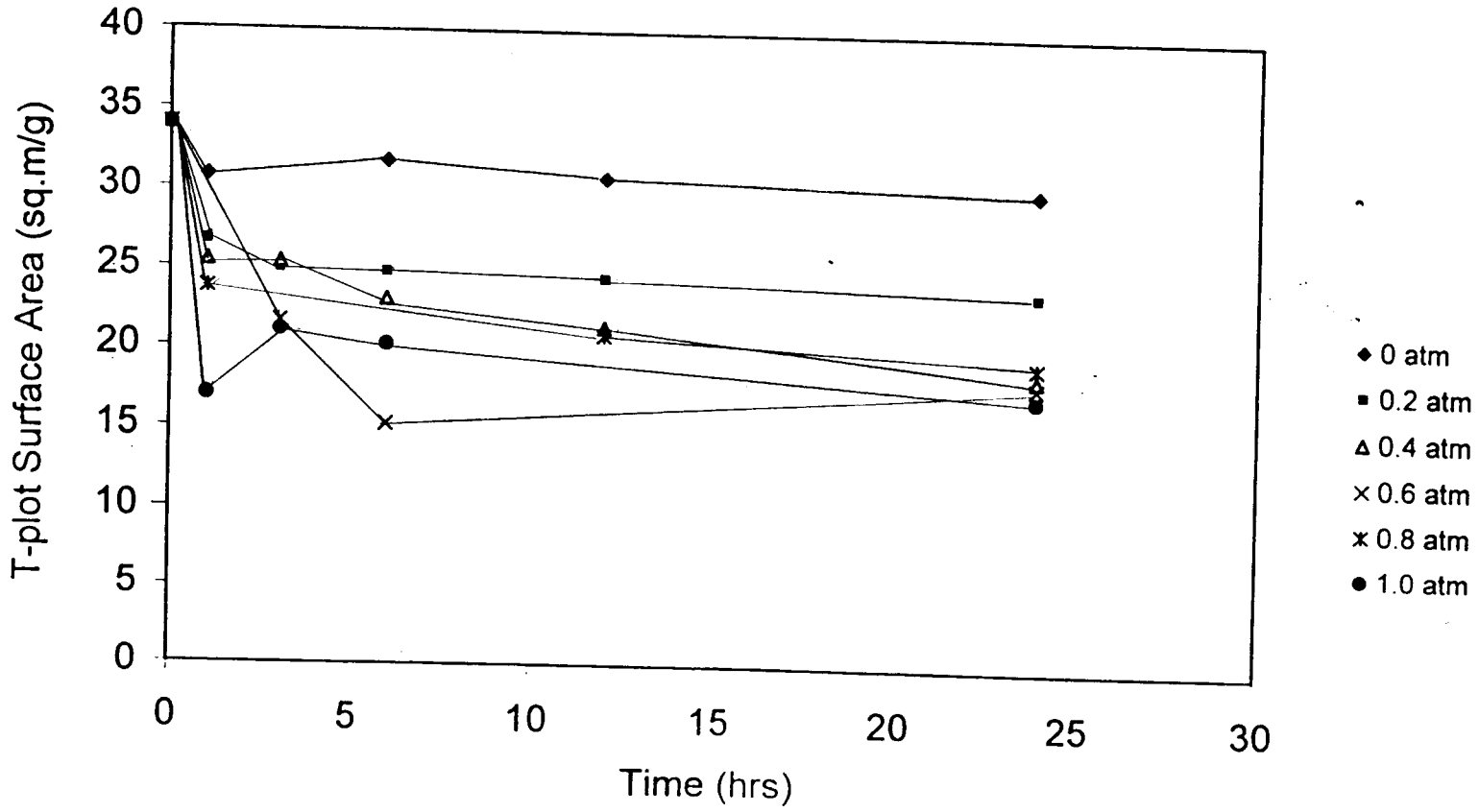

Figure 23. RE-USY t-plot surface area hydrothermal stability at 800 °C and various steam partial pressure as a function of time.

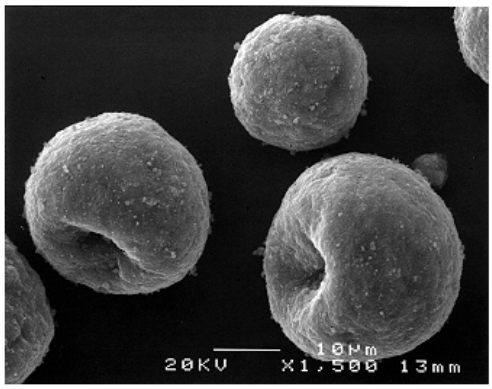

Fresh(×1500)

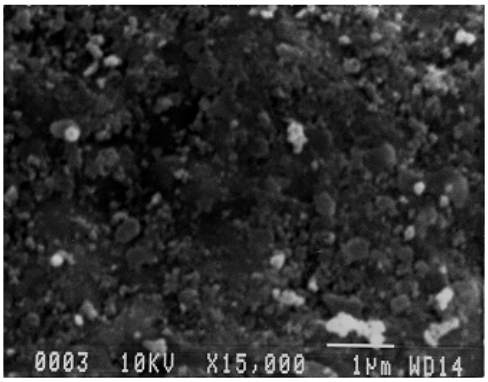

Fresh (×15000)

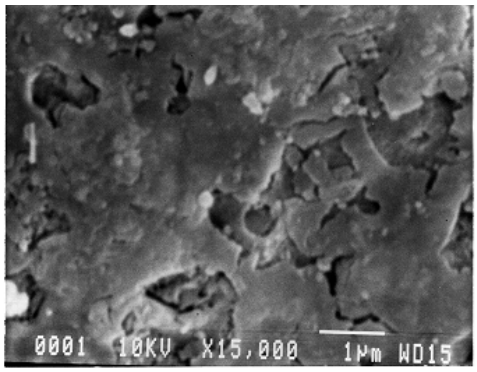

750° C 1 atm steam (×15000)

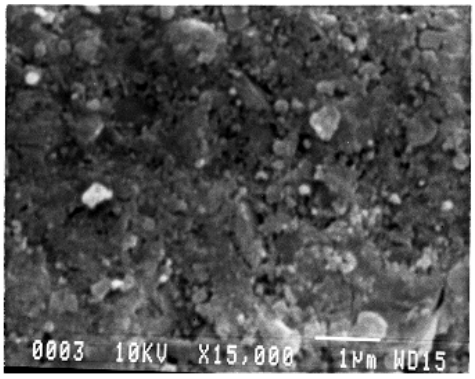

800 °C 1 atm steam (×15000)

Figure 24. Comparison of surface morphology between fresh and steam-aged RE-USY (Davidson GO-40) FCC catalyst

Based on the results of this investigation, the RE-USY (Davison GO-40) FCC catalyst exhibited much greater hydrothermal stability compared to the H-USY (Davison Octacat) catalyst. The stability of a zeolite framework is known to be related to its Si/Al ratio (1,4). Stabilization of the zeolite framework can possibly be achieved through dealumination or aluminum depletion-silicon reinsertion process with the presence of steam. However only 50%

of the aluminum atoms can be removed and replaced by silicon atoms to permanently stabilize the structure(1). Total dealumination leads to collapse of the whole zeolite structure. Since the Si/Al ratio of the H-USY and RE-USY catalyst are similar, the hydrothermal stability of the zeolite framework depends on their dealumination processes. It is known that aluminum atoms are held more firmly in the framework when associated with rare-earth ions. Therefore, the RE-USY exhibits much higher hydrothermal stability than the H-USY by preventing extraction of the aluminum atoms.

An attempt to steam deactivate for higher time (48 hrs.) has been made, the results are shown in Table 9. The reduction of the total surface area, zeolite surface area and matrix surface area of steam aged RE-USY (Davison GO-40) FCC catalyst at 750^{o}C and 0.4 atm steam partial pressure continuously occurred at a small rate.

Temp.(^{o}C)	P_{steam}(atm)	Time (hrs.)	BET SA (m^2/g)	t-Plot SA (m^2/g)	Zeolite SA (m^2/g)
750	0.4	1	248.97	30.031	218.94
750	0.4	3	235.61	28.297	207.31
750	0.4	6	230.61	27.602	203.01
750	0.4	12	225.56	26.397	199.16
750	0.4	24	219.58	25.076	194.50
750	0.4	48	209.59	24.281	185.31

Table 9. Higher time steam deactivation of the RE-USY (Davison GO-40) FCC catalyst.

In summary, Gardner's (11) structural deactivation kinetic model proved to be useful as a quantitative measure of H-USY and RE-USY zeolite hydrothermal stability. The predicted values of the zeolite surface area for both H-USY and RE-USY after being used in a hydrothermal environment can be obtained from the model.

6.0 CONCLUSIONS AND RECOMMENDATIONS

The hydrothermal aging of the RE-USY (Davison GO-40) FCC catalyst induced surface area reduction of the catalyst, including both zeolite and silica-alumina matrix. The zeolite surface area reduction for the RE-USY zeolite catalyst was found to follow the relationship developed earlier by Gardner (11) for the H-USY (Davison Octacat) FCC catalyst as

$$[(S_0-S)/S_0]^{ns} = k_{s0}e^{(-Ea/RT)}\ t$$

where S_0 is the initial surface area, S is the surface area at time t, E_A is an apparent activation energy for the zeolite hydrothermal stability, n_s is a constant which is a function of steam partial pressure for a given temperature, k_{s0} is a pre-exponential factor, t is time on stream, R is the gas constant and T is absolute temperature. The model proved to be useful as a quantitative measure of H-USY and RE-USY hydrothermal stability. The surface area prediction errors were less than six percent.

By comparison of the kinetic parameters between the H-USY and the RE-USY, the RE-USY with its smaller hydrothermal stability rate constant, K_s and smaller n_s was found to exhibit greater hydrothermal stability than the H-USY. The better hydrothermal stability of the RE-USY was suggested to be the effect of the rare-earth ion exchange to the zeolite framework. It is known that aluminum atoms are held more firmly in the zeolite framework when associated with rare-earth ion exchange, therefore the RE-USY exhibits smaller changes of the zeolite structure. The aluminum depletion of the zeolite framework also corresponds to a decrease in the number of acidic sites (1). However, only the aluminum associated with a proton can be extracted; that associated with sodium or rare-earth ions is more firmly held in the framework. Therefore, the richer the zeolite in rare-earth, the more effectively it preserves its acidic sites in the severe

hydrothermal conditions in the regenerator. The RE-Y catalyst was thought to offer not only better stability but also higher acidity compared to H-Y catalyst. It is known that rare-earth ions do not bring any acidity by themselves but protect part of the acidity (1). With these roles of the zeolite structure modification, the manufacturer can adjust the properties of the zeolite in the fresh catalysts through various processes including the rare earth ion exchange.

Based on the results obtained from this experiment, the changes in the zeolite structure occurs rapidly and significant reduction in surface area occurs within the first hour. There is a need to investigate and quantify the initial structural collapse within this period of time. The mechanism of the zeolite dealumination also needs to be investigated. Several techniques can be used such as X-ray diffraction to study unit cell parameters, ^{29}Si and ^{27}Al NMR to study Si/Al ratio and distribution of Al in different sites (T_1, T_2), IR spectroscopy to study the frequencies of the asymmetric and symmetric T-O bands, XPS to study Si/Al ratio of the outer surface (18). However, in recent years, computer simulation has become a useful tool to investigate the structural and dynamic properties of zeolites, for example, the Charge Transfer Molecular Dynamics (CTMD) computer simulations by Alvarez and co-workers (19) of a Y zeolite framework interacting with a set of Al and O ions with Si/Al ratios was found to resemble those experimentally obtained by chemical analysis and NMR studies.

In some future study, one may include investigation of the hydrothermal aging of zeolite catalysts by in-situ experiment and real time observation. The study in this thesis can be extended to evaluating the steam aged samples in a microactivity test (MAT) unit. The microactivity test provides data to assess the relative performance of equilibrium or laboratory-

deactivated fluid cracking catalyst in terms of weight percent conversion of gas oil in a microactivity unit. The activity of the catalysts can then be correlated to their hydrothermal stability. From the previous chapter, the results from higher time steam deactivation (48 hours) showed continuously decreasing in both zeolite and matrix surface area, in some future works, observation at higher steam-aging time may be interested.

Since a review of literature indicated that the ASTM method D4463-91 "Standard guide for steam deactivation of fresh fluid cracking catalysts" was rarely followed, it may need to be improved in such the way to be more flexible to deactivate different types of catalysts. Due to the large variations in properties among fresh FCC catalyst types as well as between commercial cracking unit designs and/or operating conditions, no single set of steaming deactivation conditions is adequate to artificially simulate the equilibrium catalyst for all purposes. So rather than having only steaming condition at temperature 780-810^{o}C and time of 4-6 hours, alternative conditions such as lower temperature (400-500 ^{o}C) for a longer time (24-48 hours) or higher temperature (800-1000 ^{o}C) for a short time (1-2 hours) may be included. The flexibility of steaming time is important for adjusting experimental procedures to the time schedules of individual laboratories.

7.0 Bibliography

1. Marcilly C., *The Arabian J. for Sci. and Eng.* 21 (1996), 298-311
2. Occelli L.M. and Connor P., Fluid Cracking Catalysts, Marcel Dekker: New York, 1997 p. 291
3. Bhatia S., Zeolite Catalysis: Principles and Applications, CRC Press: Boca Raton, 1990 p. 1-8, 209-249
4. Breck D.W., Zeolite Molecular Sieves: Structure, Chemistry and Use, John Wiley and Sons: New York, 1974 p. 1-5, 187, 483-528
5. Chen-Chin L., Dissertation: Deactivation Effects of Nitrogen Compounds on Lanthanum Y Zeolite, University Microfilms International: Ann Arbor, 1985 p.1-5
6. Gates B. C., Catalytic Chemistry, John Wiley and Sons: New York, 1992 p.254-276
7. Ullman's Encyclopedia of Industrial Chemistry A28 p.475-499
8. Blackmond D.G., Thesis: An In-Situ FTIR Investigation of Coke Formation on Zeolite Cracking Catalysts, University of Pittsburgh, Pittsburgh, 1981
9. Jansen J.C., Advanced Zeolite Science and Applications: Studies in Surface Science and Catalysis, Elsevier 85 (1994) p.587-628
10. Theologos K.N., Nikou I.D., Lygeros A.I. and Markatos N.C., *AIChE J.* 43 (1997) p. 486-493
11. Gardner H.T., Thesis: Irreversible Deactivation Kinetics of USY and ZSM-5 Zeolite Catalysts, (1995) WVU, Morgantown
12. Campbell S.M., Bibby D.M., Coddington J.M., Howe R.F., and Meinhold R.H., *J. of Cat.* 161 (1996) p.383-349
13. Lucas A., Canizares P. and Carrero A., *Applied Catalysis A: General* 154 91997) p.221-240

14. Kerr G.T. *J. of Phy.Chem.* 72 (1968) p. 2594-2596

15. Gallezot P., Beaumont R. and Barthomeuf D., *J. of Phy.Chem.* 78 (1974) p. 1550-1553

16. Pelmenschikov G., Paukshtis A., Edisherashvili O. and Zhidomirov M. *J. of Phy.Chem.* 96 (1992) p. 7051-7055

17. Bodart P., Nagy J., Debras G., Gabelica Z and Jacobs P. *J. of Phy.Chem.* 90 (1986) p. 5183-5190

18. Carvalho P., Ribeiro R. and Fernandez G. *Zeolites* 13 (1993) p. 462-468

19. Alvarez J., Ramirez A. and Giral B. *Zeolites* 18 (1997) 54-62

20. Sulikowski B., Borbely G. and Beyer K. *J.of Phy.Chem.* 93 (1989) p. 3240-3243

21. Miessner H., Kosslick H., Lohse U. and Tuan J. *J. of Phy.Chem.* 97 (1993) p. 9741-9748

22. Occelli L., Aurox A., Baldiraghi F. and Leoncini S. "The Use of Microcalorimetry and Porosimetry to Investigate the Effects of Aging on the Acidity of Fluid Cracking Catalysts (FCC)" Fluid Cracking Catalysts Occelli L. and Connor P. ed. Marcel Dekker: New York 1997 p. 203-215

23. ASTM D4463-91 "Standard Guide For Steam Deactivation of Fresh Fluid Cracking Catalyst"

24. Moorehead L., Margolis J. and Mclean B. "Evaluation of Fluid Cracking Catalysts: A Comparative Study of Testing Philosophies" Characterization and Catalyst Development: An Interactive Approach. Bradley A., Gattuso J. and Beertolacini J. ACS Symposium Series 411, 1989 p. 120-134

25. McElhiney G. *Oil and Gas J.* Feb. 8 (1988) p. 35-36

26. ASTM D3907-87 "Standard Method for Testing Fluid Cracking Catalysts by Microactivity Test"

27. Keyworth A., Turner J. and Reid A. *Oil and Gas J.* Mar. 14 (1988) p. 656-68

28. Mclean B., and Moorehead L. *Hydrocarbon processing* Feb. (1991) p. 41-45

29. Magee S. and Blazek J. Zeolite Chemistry and Catalysis Ed. Robo J. ACS monograph 171 (1976) p. 615-679

30. Scherzer J. and Bass L. *J. of Cat.* 28 (1973) p. 101-115

31. Kerr T., *J. of Cat.* 15 (1969) p. 200-204

32. Basacek V. and Patzelova V. "Stabilized Y Zeolites:Preparation and Properties" Catalysis on Zeolites, Kallo D. and Minachev M. Ed.: Stillman 1988 p. 169-181

33. Yates G., Fundamentals of Fluidized-Bed Chemical Processes, 1983 Butterworths: London p. 32-33

34. Wang L., Gianetto G., Torrealba M. and Kappenstein C. *J. of Cat.* 130 (1991) p. 459-470

35. Pellet R., Blackwell S. and Rabo A. *J. of Cat.* 114 (1998) p. 71-89

36. Schaffer G., Adams R. and Wilson N., *J. of Phy.Chem.* 69 (1965) p. 1530-1536

37. Chen. Y., Mitchell O., Olson H. and Peirine B. Ind. Eng. and Chem.Prod. Res. and Dev. 16 (1977) p. 247-252

38. Chester W., and Stover A. *Ind.Eng.and Chem.Prod.Res. and Dev.* 16 (1977) p. 285-290

39. Suckow M., Lutz W., Kornatowski J., Rozwadowski M. and Wark M., *Gas Separation and Purification* 6 (1992) p. 101-108

40. Blasco V., Royo C., Monzon A. and Santamaria J. *AIChE J.* 38 (1992) p. 237-242

41. Gregg S. J., Sing K. S. W., Adsorption, Surface Area and Porosity 2nd edition, Academic Press, New York, 1982.

42. ASTM D 3363-92 "Standard Test Method for Surface Area of Catalysts"

43. ASTM D 4365-85 (Reapproved 1994) “Standard Test Method for Determining Zeolite Area of a catalyst”

44. Coulter Omnisorp Manual, Coulter Corporation, Haileah, Florida.

APPENDIX A

BET and t-plot surface area data of steam aged RE-USY (Davison GO-40) FCC catalyst

Temp.(°C)	P_{steam}(atm)	Time (hrs)	BET(m^2/g)	t-Plot(m^2/g)	Zeolite(m^2/g)
Fresh 1	-	-	280.34	35.898	244.44
Fresh 2	-	-	273.93	32.136	241.79
Fresh 3	-	-	273.75	31.421	242.33
Fresh 4	-	-	269.84	31.229	238.61
Fresh 5	-	-	269.56	30.102	239.46
Fresh 6	-	-	274.11	32.850	241.26
Fresh (avg.)	-	-	273.59	32.273	241.32
500	0	1	271.10	36.137	234.96
500	0	3	272.99	37.048	235.94
500	0	6	266.26	32.557	233.70
500	0	12	266.37	33.312	233.06
500	0	24	265.64	33.804	231.84
550	0	12	263.93	34.970	228.96
550	0.1	3	265.5	31.488	234.01
550	0.1	6	264.29	30.942	233.35
550	0.1	24	264.28	32.461	231.82
550	0.2	3	260.98	30.268	230.71
550	0.2	6	268.48	33.552	234.93
550	0.2	12	269.67	32.927	236.74
550	0.2	24	268.98	32.861	236.12
550	0.4	3	253.4	32.556	220.84
550	0.4	6	271.13	33.207	237.92
550	0.4	24	243.7	33.23	210.47
550	0.6	3	253.51	32.728	220.78
550	0.6	6	249.05	33.844	215.21
550	0.6	12	244.13	33.206	210.92
550	0.8	3	248.75	31.131	217.62
550	0.8	12	245.04	32.042	213.00
550	0.8	24	243.61	30.558	213.05
550	1.0	6	247.63	31.237	216.39
550	1.0	24	244.86	28.524	216.34

Temp.(°C)	P_{steam}(atm)	Time (hrs)	BET(m^2/g)	t-Plot(m^2/g)	Zeolite(m^2/g)
600	0	1	261.9	32.479	229.42
600	0	3	260.95	33.341	227.61
600	0	6			
600	0	12	260.28,258.94	33.595,30.388	226.68,228.55
600	0	24	259.60	32.122	227.478
600	0.1	1			
600	0.1	3	257.77	32.604	225.17
600	0.1	6	259.62	30.530	229.09
600	0.1	12	259.70	30.437	229.26
600	0.1	24	254.25	32.398	221.85
600	0.2	1			
600	0.2	3	260.41	31.161	229.249
600	0.2	6	260.19	31.151	229.04
600	0.2	12	261.77	31.103	230.67
600	0.2	24	259.44	31.815	227.625
600	0.3	1			
600	0.3	3	261.88	30.354	231.53
600	0.3	6	260.36	30.710	229.65
600	0.3	12	261.27	31.675	229.59
600	0.3	24			
600	0.4	1			
600	0.4	3	253.02	31.771	221.249
600	0.4	6	251.21	31.655	219.555
600	0.4	12	248.12	30.546	217.574
600	0.4	24	247.15	32.335	214.815
600	0.6	1			
600	0.6	3	255.07	31.494	223.576
600	0.6	6	252.45	31.914	220.536
600	0.6	12	244.22	30.799	213.421
600	0.6	24	243.19	30.234	212.956
600	0.8	1	256.45	31.801	224.649
600	0.8	3	254.16	31.910	222.25
600	0.8	6	247.15	32.154	214.996
600	0.8	12	243.69,245.88	30.335,30.445	213.35,215.43
600	0.8	24	240.50,242.66	29.028,30.204	211.47,212.46

Temp.(°C)	P_{steam}(atm)	Time (hrs)	BET (m^2/g)	t-Plot (m^2/g)	Zeolite(m^2/g)
600	1.0	1	258.63	31.089	227.541
600	1.0	3	242.45,245.47,241.68	31.121,31.386,28.171	211.33,214.08
600	1.0	6	252.65	32.014	220.636
600	1.0	12	247.97	31.208	216.672
600	1.0	24	247.34	32.170	215.17
650	0	1	260.48	32.722	228.558
650	0	3	259.04	34.517	224.523
650	0	6	258.12	31.064	227.056
650	0	12	259.24	33.311	225.929
650	0	24	257.89	33.773	224.117
650	0.2	1	259.10	32.602	226.498
650	0.2	3	257.81	32.01	225.8
650	0.2	6	257.77	29.172	228.598
650	0.2	12	255.58	31.84	223.74
650	0.2	24	256.15	31.192	224.958
650	0.4	1	257.14	31.697	225.443
650	0.4	3	255.47	28.100	227.37
650	0.4	6	253.15	29.168	223.982
650	0.4	12	252.90	29.510	223.39
650	0.4	24	248.34	28.416	219.924
650	0.6	1	248.67	31.117	217.55
650	0.6	3	251.85	30.026	221.824
650	0.6	6	249.60	29.508	220.092
650	0.6	12	247.91	28.846	219.064
650	0.6	24	243.55	29.389	214.161
650	0.8	1	250.83	29.790	221.04
650	0.8	3	237.35	26.911	210.44
650	0.8	6	246.55	28.356	218.194
650	0.8	12	226.71	26.915	199.795
650	0.8	24	246.78	26.190	220.59
650	1.0	1	248.32	27.623	220.697
650	1.0	3	244.70	28.096	216.604
650	1.0	6	260.00	28.227	231.67
650	1.0	12	237.81	28.014	209.796
650	1.0	24	238.05	26.630	211.42

Temp.(°C)	P_{steam} (atm)	Time (hrs)	BET (m^2/g)	t-Plot (m^2/g)	Zeolite(m^2/g)
700	0	1	256.63	32.385	224.245
700	0	3	253.82	29.253	224.57
700	0	6	255.72	30.528	225.197
700	0	12	255.63	31.481	224.145
700	0	24	256.05	33.187	222.863
700	0.2	1	253.57	33.585	219.985
700	0.2	3	259.52	31.822	227.698
700	0.2	6	259.82	31.779	228.041
700	0.2	12	257.21	31.915	225.295
700	0.2	24	255.33	31.885	223.445
700	0.4	1	251.25,244.25	27.832,32.603	223.42,211.65
700	0.4	3	263.82	31.607	232.21
700	0.4	6	252.34	32.819	219.521
700	0.4	12	252.87	32.571	220.299
700	0.4	24	241.38	31.731	209.649
700	0.6	1	242.12	32.333	209.79
700	0.6	3	253.81	31.492	222.318
700	0.6	6	248.31	32.792	215.518
700	0.6	12	248.36	30.654	217.706
700	0.6	24	245.24	31.674	213.566
700	0.8	1	240.82,244.29	27.475,30.692	213.35,213.59
700	0.8	3	240.0,241.54	26.331,27.244	213.67,214.3
700	0.8	6	245.68,256.13,228.32	25.241,32.813,26.618	220.44,201.7
700	0.8	12	228.67,238.04	26.152,30.102	202.52,207.94
700	0.8	24	231.79,232.04	26.182,28.430	205.61,203.61
700	1.0	1	238.64	28.029	210.671
700	1.0	3	243.38	29.349	214.03
700	1.0	6	232.56	26.249	206.311
700	1.0	12	234.82	29.283	205.537
700	1.0	24	220.03	24.861	195.169
750	0	1	256.90	26.777	230.123
750	0	3	254.47	31.882	222.588
750	0	6	251.87,266.68	28.521,27.181	239.5
750	0	12	253.38	31.376	222.004
750	0	24	254.71	31.318	223.392

Temp.(°C)	P_{steam}(atm)	Time (hrs)	BET(m^2/g)	t-Plot(m^2/g)	Zeolite(m^2/g)
750	0.2	1	257.81	30.363	227.447
750	0.2	3	255.12	31.237	223.883
750	0.2	6	254.98	31.326	223.654
750	0.2	12	252.23	30.490	221.74
750	0.2	24	249.88	31.211	218.669
750	0.4	1	248.97	30.031	218.939
750	0.4	3	235.61	28.297	207.313
750	0.4	6	230.61	27.602	203.008
750	0.4	12	225.56	26.937	198.623
750	0.4	24	219.58	25.076	194.504
750	0.6	1	241.51	27.046	214.464
750	0.6	3	228.49	27.169	201.321
750	0.6	6	234.52	27.623	206.897
750	0.6	12	216.79	24.009	192.781
750	0.6	24	212.86	22.959	189.901
750	0.8	1	242.36	28.648	213.712
750	0.8	3	233.51	28.692	204.818
750	0.8	6	235.72	26.429	209.291
750	0.8	12	226.18	24.199	201.981
750	0.8	24	221.85	26.186	195.664
750	1.0	1	227.91	22.285	205.625
750	1.0	3	220.78,246.83	22.880,29.528	197.9,217.3
750	1.0	6	218.45,234.47	23.031,27.104	195.42,207.37
750	1.0	12	233.22,223.91	28.45,26.335	204.77,197.57
750	1.0	24	202.08,205.83	22.278,21.422	179.80,184.41
800	0	1	254.01	30.779	223.231
800	0	3	248.10	27.550	220.55
800	0	6	253.33	31.758	221.572
800	0	12	250.92	30.804	220.116
800	0	24	254.09	30.183	223.907
800	0.1	1	227.97	25.897	202.07
800	0.1	3	231.4	29.428	201.97
800	0.1	6	215.96	20.476	195.48
800	0.1	12	210.15	24.481	185.67
800	0.1	24	203.36	23.47	179.89

Temp.(°C)	P_{steam}(atm)	Time (hrs)	BET(m^2/g)	t-Plot(m^2/g)	Zeolite(m^2/g)
800	0.2	1	232.83	26.685	206.145
800	0.2	3	229.33	24.941	204.389
800	0.2	6	228.29	24.794	203.496
800	0.2	12	220.94	24.492	196.448
800	0.2	24	214.56	23.757	190.803
800	0.4	1	226.44	25.443	200.997
800	0.4	3	225.89	25.371	200.519
800	0.4	6	212.10	23.069	189.031
800	0.4	12	206.04	21.416	184.624
800	0.4	24	192.84	18.564	174.276
800	0.6	1	247.68,217.76	30.194,22.936	217.49,194.82
800	0.6	3	210.47	21.637	188.833
800	0.6	6	172.96	18.477	154.48
800	0.6	12	166.92	15.239	151.681
800	0.6	24	169.80	18.062	151.738
800	0.8	1	219.45,235.26	23.727,26.162	195.723,209.1
800	0.8	3	237.49,204.75	21.378,21.517	216.11,183.23
800	0.8	6	224.03,190.57	25.210,18.682	198.82,171.89
800	0.8	12	190.27	20.908	169.362
800	0.8	24	175.46	19.300	156.16
800	1.0	1	197.64	23.727	173.913
800	1.0	3	198.74	21.074	177.666
800	1.0	6	194.0	20.221	173.779
800	1.0	12	172.32	16.993	155.327
800	1.0	24	162.49	17.212	145.278

APPENDIX B

BET and t-plot surface area data of steam aged H-USY (Davison Octacat) FCC catalyst (original data from Gardner's (11)

Temp. (°C)	P_{steam} (atm)	Time (hrs)	BET SA (m^2/g)	t-Plot SA (m^2/g)
Fresh 1-	-		277.82	43.012
650	0	1	267.20	34.0
650	0	3	270.90, 271.1	42.097, 29.4
650	0	6	266.5	31.8
650	0	12	265.0	30.5
650	0	24	266.7	31.8
650	0.2	1	258.9	43.8
650	0.2	3	250.0	44.6
650	0.2	6	248.74, 245.1	40.3
650	0.2	12	242.48, 241.7	34.6
650	0.2	24	241.61, 238.0	41.588, 33.4
650	0.4	1	251.82	49.270
650	0.4	3	246.30, 242.7	44.467, 40.1
650	0.4	6	238.86	46.141
650	0.4	12	236.38	47.299
650	0.4	24	233.06	45.127
650	0.6	1	246.34	46.001
650	0.6	3	238.80	46.431
650	0.6	6	235.15	45.541
650	0.6	12	233.01	44.761
650	0.6	24	228.69	45.401
650	0.8	1	242.46	45.542
650	0.8	3	237.11, 233.4	43.345, 34.9
650	0.8	6	233.26	45.774
650	0.8	12	229.50	45.827
650	0.8	24	222.46	45.492

Temp. (°C)	P_{steam} (atm)	Time (hrs)	BET SA (m^2/g)	t-Plot SA (m^2/g)
650	1.0	1	239.33	45.444
650	1.0	3	231.82	48.064
650	1.0	6	228.71, 229.4	40.684, 33.9
650	1.0	12	220.87	43.705
650	1.0	24	218.49	44.817
700	0	1	271.79, 267.9	43.311, 29.2
700	0	3	265.4	31.3
700	0	6	264.1	34.7
700	0	12	261.5	31.3
700	0	24	261.2	32.4
700	0.2	1	251.00	43.720
700	0.2	3	247.92, 246.0	43.361, 35.2
700	0.2	6	236.2, 240.4	33.6, 35.4
700	0.2	12	236.24	43.330
700	0.2	24	229.1	35.1
700	0.4	1	247.52, 241.2	43.834, 33.8
700	0.4	3	235.6	34.4
700	0.4	6	235.92	38.501
700	0.4	12	228.04	43.295
700	0.4	24	223.00	41.131
700	0.6	1	242.26	40.768
700	0.6	3	-	-
700	0.6	6	226.44, 227.0	29.496, 34.1
700	0.6	12	-	-
700	0.6	24	-	-
700	0.8	1	234.00	46.423
700	0.8	3	-	-
700	0.8	6	-	-
700	0.8	12	220.30	41.265
700	0.8	24	214.8	29.8
700	1.0	1	234.26	47.719
700	1.0	3	-	-
700	1.0	6	-	-
700	1.0	12	216.17	43.351
700	1.0	24	211.7	35.8

Temp. (°C)	P_{steam} (atm)	Time (hrs)	BET SA (m^2/g)	t-Plot SA (m^2/g)
750	0	1	270.39	38.894
750	0	3	268.99	40.999
750	0	6	267.97	43.389
750	0	12	265.90	43.972
750	0	24	260.96	42.821
750	0.2	1	243.79	40.402
750	0.2	3	-	-
750	0.2	6	232.00	42.089
750	0.2	12	221.53	41.158
750	0.2	24	212.49	38.276
750	0.4	1	234.84, 233.5	31.262, 31.3
750	0.4	3	233.45, 232.4	40.731, 35.9
750	0.4	6	225.56	40.584
750	0.4	12	220.21, 220.6	37.688, 34.8
750	0.4	24	213.87	40.235
750	0.6	1	235.29, 232.7	38.614, 34.4
750	0.6	3	224.72	42.616
750	0.6	6	222.55	42.055
750	0.6	12	214.39, 216.3	34.954, 35.4
750	0.6	24	208.67, 211.0	32.733, 33.8
750	0.8	1	231.06	43.213
750	0.8	3	-	-
750	0.8	6	216.89	38.777
750	0.8	12	213.48	35.513
750	0.8	24	207.87	39.411
750	1.0	1	229.93	42.941
750	1.0	3	221.85	40.817
750	1.0	6	215.71	38.839
750	1.0	12	209.05	35.722
750	1.0	24	203.52	38.186
800	0	1	256.47, 260.3	38.421, 28.9
800	0	3	256.18	49.976
800	0	6	251.61	46.068
800	0	12	235.07	36.873
800	0	24	238.06	40.766

Temp. (°C)	P_{steam} (atm)	Time (hrs)	BET SA (m^2/g)	t-Plot SA (m^2/g)
800	0.2	1	236.85	44.462
800	0.2	3	225.23	41.638
800	0.2	6	219.95	43.316
800	0.2	12	210.43	40.991
800	0.2	24	211.56, 215.2	43.254, 32.8
800	0.4	1	225.44	38.839
800	0.4	3	219.97	40.866
800	0.4	6	205.35	32.547
800	0.4	12	204.19	41.292
800	0.4	24	193.59, 198.2	29.878, 21.4
800	0.6	1	220.80, 221.3	44.619, 32.6
800	0.6	3	211.01	36.862
800	0.6	6	211.75, 208.0	37.408, 29.5
800	0.6	12	194.60	39.475
800	0.6	24	190.40, 191.8	36.377, 31.3
800	0.8	1	216.41, 218.9	33.095, 35.4
800	0.8	3	203.02	38.369
800	0.8	6	193.99	38.198
800	0.8	12	186.27	33.686
800	0.8	24	176.08, 179.6	36.044, 30.8
800	1.0	1	210.82, 213.0	30.876, 29.4
800	1.0	3	200.06, 204.1	39.109, 32.1
800	1.0	6	193.58	39.315
800	1.0	12	184.90	35.679
800	1.0	24	168.41, 171.5	28.962, 29.5

APPENDIX C

Surface area best fit parameters for the H-USY (Davison Octacat) FCC catalyst.

Temp.(°C)	E_A (J/mol)	k_{s0} (hr^{-1})	n_s
650	95,310	1.163×10^3	$n_s = 3.305+4.36P_{steam}^{0.36}$
700	95,310	1.163×10^3	$n_s = 3.111+4.14P_{steam}^{0.36}$
750	95,310	1.163×10^3	$n_s = 3.064+4.269P_{steam}^{0.17}$
800	95,310	1.163×10^3	$n_s = 4.075+4.466P_{steam}^{0.43}$

APPENDIX D

Deactivation kinetic parameters ; K_s and n_s for hydrothermal aging of the H-USY (Davison Octacat) FCC catalyst.

Temp. (oC)	Psteam (atm)	Ks (hr-1)	n_s
650	0	2.305E-03	3.31
	0.2	2.305E-03	5.75
	0.4	2.305E-03	6.44
	0.6	2.305E-03	6.93
	0.8	2.305E-03	7.33
	1.0	2.305E-03	7.67
700	0	4.694E-03	3.11
	0.2	4.694E-03	5.43
	0.4	4.694E-03	6.09
	0.6	4.694E-03	6.56
	0.8	4.694E-03	6.93
	1.0	4.694E-03	7.25
750	0	8.887E-03	3.06
	0.2	8.887E-03	6.31
	0.4	8.887E-03	6.72
	0.6	8.887E-03	6.98
	0.8	8.887E-03	7.17
	1.0	8.887E-03	7.33

Temp. (oC)	Psteam (atm)	Ks (hr-1)	ns
800	0	1.581E-02	4.08
	0.2	1.581E-02	6.31
	0.4	1.581E-02	7.09
	0.6	1.581E-02	7.66
	0.8	1.581E-02	8.13
	1.0	1.581E-02	8.54

APPENDIX E.

Procedure for calculation of K_s, k_{s0}, E_A and n_s

(for the RE-USY (Davison GO-40) FCC catalyst data)

1. Select a consistent set of data

   For example: data at 750 °C and 0.6 atm steam partial pressure

   from the surface area reduction model

   $[(S_0-S)/S_0]^{ns} = K_s t$

   Rewrite the equation in a logarithm form

   $n_s \log[(S_0-S)/S_0] = \log (K_s) + \log (t)$

   or $\log (t) = n_s \log[(S_0-S)/S_0] - \log K_s$

2. Plot log (t) versus $\log[(S_0-S)/S_0]$ (Figure 25)

   slope = n_s = 3.79

   intercept = $-\log(K_s)$

   $K_s = 1.68 \times 10^{-4}$ hr^{-1}

3. Plotting log (t) versus $\log[(S_0-S)/S_0]$ for every consistent data set (T, P)

   gives the K_s and n_s values at any T, P

   Average the K_s value at a given temperature then E_A can be calculated from any two

   values of K_s by the equation

   $K_s = k_{s0} e^{-Ea/RT}$

4. Average the apparent activation energy, E_A since it appeared to be constant.

5. k_{s0} can be calculated for any K_s by the same equation using the average E_A (for Method 2)

6. k_{s0} shows large variation with temperature and steam partial pressure, however by assuming k_{s0} constant (using the average value), and re-calculate K_s using equation $K_s = k_{s0}e^{-Ea/RT}$ (Method1)

   The K_s value did not appear much different from the average value in method 2. Therefore, method 1 (k_{s0} and E_A constant) was satisfied while method 2 (k_{s0} varied) did not appear to be satisfied due to the inconsistent value of k_{s0}

7. Calculation of n_s

   By keeping K_s constant at a given temperature, n_s were calculated based on selected data using the model equation.

$$\log (t) = n_s \log[(S_0-S)/S_0] - \log (K_s)$$

6. Writing n_s equation as a function of P_{steam}

   by plotting n_s versus P_{steam} (Figure 26), the relationship between n_s and P_{steam} was determined to be a linear relationship.

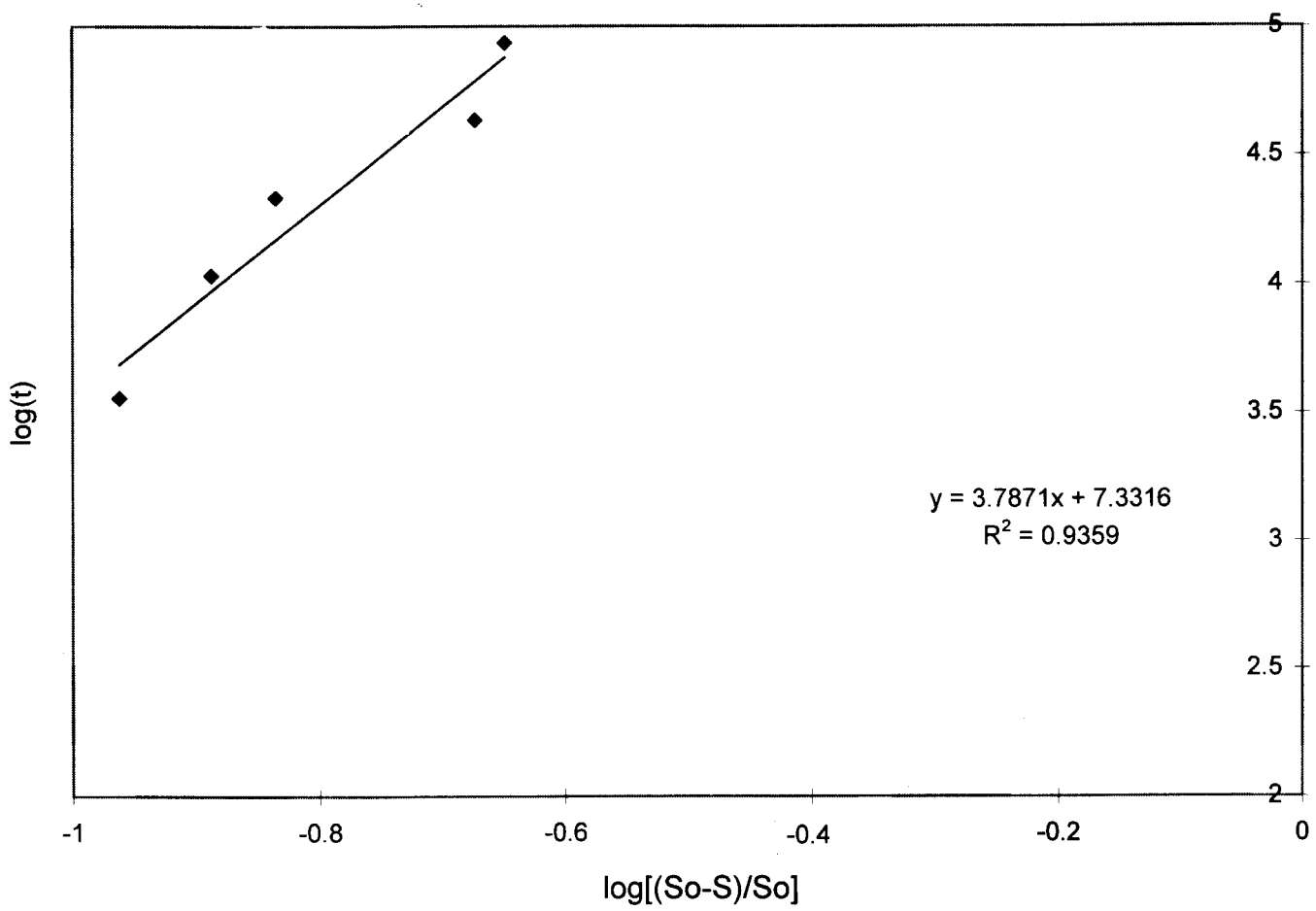

Figure 25. Plotting of log(t) vs. log [(So-S)/So using data at T=750°C , P_{steam} = 0.6

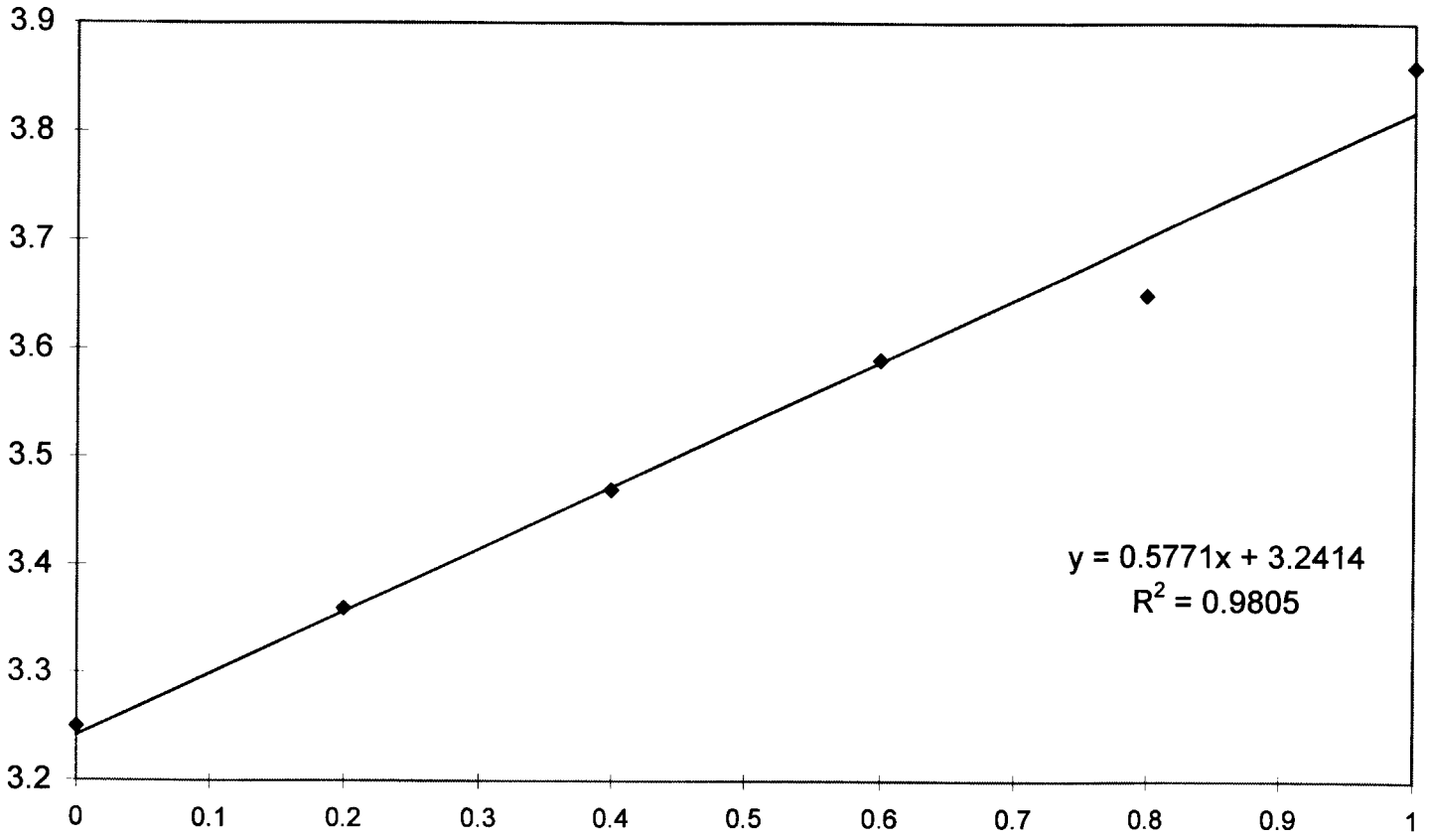

Figure 26. Plotting n_s vs. P_{steam} using data at T=600 °C

HYDROTHERMAL AGING OF ZEOLITE-BASED CATALYSTS

By
Joongjai Panpranot

A THESIS

Submitted to
The College of Engineering and Mineral Resources

at
West Virginia University

in partial fulfillment of the requirements
for the degree of Master of Science

in
Chemical Engineering

Department of Chemical Engineering

Morgantown, West Virginia
1998

_____
Edwin L. Kugler, Ph.D.

_____
Charter D. Stinespring, Ph.D.

_____
Dady B. Dadyburjor, Ph.D.